

1 **A multidisciplinary study of ecosystem evolution through early**
2 **Pleistocene climate change from the marine Arda River section (Italy)**

3 **Gaia Crippa ^a, Andrea Baucon ^{b, c}, Fabrizio Felletti ^a, Gianluca Raineri ^d and Daniele Scarponi ^e**

4

5 *^a Università degli Studi di Milano, Dipartimento di Scienze della Terra 'A. Desio', via Mangiagalli 34,*
6 *Milano, 20133, Italy. Corresponding author: gaia.crippa@unimi.it, +39 - 02503 15527*

7 *^b Università di Modena, Dipartimento di Chimica e Scienze Geologiche, Via Campi 103, 41125*
8 *Modena, Italy.*

9 *^c Geology and Palaeontology Office, Geopark Naturtejo da Meseta Meridional – UNESCO Global*
10 *Geopark. Municipality of Idanha-a-Nova – Centro Cultural Raiano. Av. Joaquim Morão, 6060-101*
11 *Idanha-a-Nova, Portugal.*

12 *^d Parco Regionale dello Stirone e del Piacenziano, Loc. Scipione Ponte 1, Salsomaggiore Terme,*
13 *43039, Italy*

14 *^e Università di Bologna, Dipartimento di Scienze Biologiche, Geologiche e Ambientali, Via Zamboni*
15 *67, Bologna, 40126, Italy*

16

17 **ABSTRACT**

18 The Arda River marine succession (Italy) represents an excellent site to apply an integrated approach to
19 palaeoenvironmental reconstructions, combining the results of sedimentology, body fossil
20 palaeontology and ichnology, to unravel the sedimentary evolution of a complex marine setting in the
21 frame of early Pleistocene climate change and tectonic activity. The succession represents a
22 subaqueous extension of a fluvial system, originated during phases of advance of fan deltas affected by
23 high-density flows triggered by river floods, and overlain by continental conglomerates indicating a

24 relative sea level fall and the establishment of a continental environment. An overall regressive trend is
25 observed through the section, from a prodelta to a delta front and intertidal settings. The hydrodynamic
26 energy and the sedimentation rate are not constant through the section, but they are influenced by
27 hyperpycnal flows, whose sediments are mainly supplied by an increase in the Apennine uplift and
28 erosion, especially after 1.80 Ma. The Arda section documents the same evolutionary history of coeval
29 successions in the Palaeo-Adriatic region, as well as the climatic changes of the early Pleistocene. The
30 different approaches used complement quite well one another, giving strength and robustness to the
31 obtained results.

32

33 *Keywords:* early Pleistocene; Facies analysis; Body fossils; Trace fossils; Palaeo-Adriatic

34

35 **INTRODUCTION**

36 The complex interactions between organisms and their environments are an important aspect of the
37 planet evolution. Biotic and abiotic systems evolve in time and leave tracks in the biosedimentary
38 record (e.g., Kowalewski et al., 2015; Wysocka et al., 2016; Martinelli et al., 2017; Scarponi et al.,
39 2017a,b). However, unfolding such a record to pinpoint how ecosystems changed in time responding to
40 palaeoenvironmental modifications requires a multidisciplinary approach including a well-established
41 stratigraphic framework, a careful taxonomy and a comprehensive ecological background (Dodd and
42 Stanton, 1990). The basic data for palaeoecology are body fossils, adequately identified, and trace
43 fossils, which record the behavioral patterns of organisms through time, both correctly positioned
44 within the stratigraphic framework. Though such a multidisciplinary approach is widely recognised to
45 be powerful in reconstructing palaeoecosystems and their evolution, it is seldom implemented in the
46 literature.

47 The lower Pleistocene marine succession of the Arda River (northern Apennines, Italy), represents an
48 excellent site where to apply multidisciplinary investigations (Crippa et al., 2016). The wealth of
49 sedimentary structures and the excellent preservation of body and trace fossils make this marine
50 succession a case study where we can integrate the abiotic and biotic components to resolve past
51 ecosystems dynamics within a key-time interval of climate change.

52 The early Pleistocene was characterised by climatic oscillations related to glacial/interglacial cycles,
53 with the Mediterranean area being affected by these changes in both marine and continental settings
54 (e.g., Bertini, 2010; Fusco, 2010; Scarponi et al., 2014; Combourieu-Nebout et al., 2015; Crippa et al.,
55 2016; von Leesen et al., 2017). The most important biotic events recorded in the marine environment of
56 the Mediterranean are the disappearance of taxa of subtropical affinity and the occurrence of “northern
57 guests”, i.e. organisms presently living at higher latitudes in the Northern Hemisphere, such as the
58 bivalve *Arctica islandica* and the foraminifera *Hyalinea balthica* and *Neogloboquadrina pachyderma*
59 left-coiling, which migrated into the entire Mediterranean Sea through the Strait of Gibraltar during
60 glacial periods since the Calabrian (early Pleistocene) (Suess, 1883–1888; Raffi, 1986; Martínez-
61 García et al., 2015). Recently, by analysing the isotopic composition of the bivalve shells from the
62 Arda River section, Crippa et al. (2016) observed that seawater temperature seasonality was the main
63 variable of climate change within the study area during the early Pleistocene, in turn controlled by the
64 Northern Hemisphere Glaciation dynamics. In particular, strong seasonality and low winter
65 palaeotemperatures were assumed to be the main drivers for the widespread establishment of “northern
66 guests” populations in the Palaeo-Adriatic Sea.

67 Here, we pursue an integrated approach involving facies analyses and palaeoecological observations to
68 investigate the relationships between body and trace fossils and their environment in the early
69 Pleistocene of the Arda Section. The purpose of this paper is twofold: first, to compare the results of
70 the analyses of sedimentology, body and trace fossils, evaluating to which extent these three different

71 approaches complement one another and derive general implications for their combined use; second, to
72 reconstruct the palaeoenvironmental evolution of the Arda River sedimentary succession comparatively
73 based on the integration of three different tools and to interpret it taking into account the interplay
74 between tectonic and climatic factors (both local and global).

75

76 **GEOLOGICAL SETTING**

77 The Arda River section is located in northern Italy near the town of Castell'Arquato at the margin of
78 the northern Apennines facing the Po plain (Fig. 1). The northern Apennines are an orogenic wedge
79 which started to form since the Oligocene as a result of the collision between the Corsica-Sardinia
80 microplate and the Adria promontory, following the closure of the Mesozoic Ligurian-Piedmont Ocean
81 (Carminati and Doglioni, 2012). Deformation migrated through time toward the east-northeast,
82 gradually involving the Ligurid oceanic units and the Adria continental margin.

83 The Arda River section belongs to the Castell'Arquato basin, a small wedge-top basin developed since
84 the Messinian (Miocene) at the eastern edge of the northern Apennine orogenic wedge as a result of the
85 fragmentation of the Po Plain foredeep (Roveri and Taviani, 2003; Artoni et al., 2010) (Fig. 1). It forms
86 part of the northwestern extension of the Palaeo-Adriatic Sea and is bounded to the north by the
87 Cortemaggiore thrust and to the south by the emerged front of Ligurid units (Monegatti et al., 2001)
88 (Fig. 1A). Several basin-wide, unconformity-bounded sedimentary cycles, recognised both on the
89 outcrops and in the subsurface of the Po Plain and the central Adriatic Sea, characterise the basin infill
90 (Pieri, 1983; Ori et al., 1986; Ricci Lucchi, 1986). The Castell'Arquato basin is filled by a sedimentary
91 succession of late Messinian (upper Miocene) to Holocene age, organized in a large-scale
92 transgressive-regressive cycle controlled by tectonics, with beds forming a regular monocline dipping
93 towards the north-northeast (Monegatti et al., 2001). The basal part of the filling succession comprises
94 deep sea sediments postdating the Messinian salinity crisis (Ceregato et al., 2007; Calabrese and Di

95 Dio, 2009), when marine conditions were restored in the Mediterranean Sea; upward they pass into
96 slope and shelf facies associations and then through a regressive trend to the middle Pleistocene
97 alluvial continental deposits, which represent the final retreat of the sea in this area and the
98 establishment of a continental environment with vertebrate faunas and freshwater molluscs (Cigala
99 Fulgosi, 1976; Pelosio and Raffi, 1977; Ciangherotti et al., 1997). Detailed studies carried out in recent
100 years through the integration of surface and subsurface data resulted in a comprehensive stratigraphic
101 and evolutive model of the Castell'Arquato basin during the Pliocene and the early Pleistocene (Roveri
102 et al., 1998; Monegatti et al., 2001; Roveri and Taviani, 2003). Insights into the palaeogeography of the
103 Po basin at the first major regression of the coastline in consequence of the lowstand during the late
104 early Pleistocene climate turnover (EPT), have been recently provided in Fig. 8 of Monesi et al. (2016).
105 The studied succession crops out along the Arda River and extends downstream the bridge located at
106 the entrance of the town of Castell'Arquato (northern Italy) (Fig. 1B, C); the marine part, which is the
107 subject of the present study, is 237 m thick and bounded at the top (44°52'9.95"N; 9°53'1.35"E) by
108 continental conglomerates (Fig. 2). The lowermost portion of the section is cut by a fault (Figs. 1B and
109 2), causing the repetition of the first 36 m of the succession (base at 44°51'18.52"N; 9°52'26.7"E); the
110 succession described here begins stratigraphically above the fault. The Arda River marine succession
111 has a Calabrian (early Pleistocene) age, ranging from ~1.8 to 1.2 Ma, based on magnetostratigraphy
112 (Monesi et al., 2016), and calcareous nannofossil and foraminifera biostratigraphy, which allowed
113 identifying respectively three nannofossil (CNPL7, CNPL8 and CNPL9) and one foraminiferal
114 (*Globigerina cariacensis*) biozones (Crippa et al., 2016).

115

116 **MATERIALS AND METHODS**

117 **Sedimentology**

118 The Arda River section has been measured bed-by-bed at 1 cm resolution. Bed thickness measurements
119 were performed mainly with a Jacob's staff (e.g., a 1.5 metre high rod equipped with a clinometer and a
120 flat sighting disc on top). The log was measured, recording the internal subdivisions of the individual
121 beds or "depositional intervals" (i.e., depositional divisions or bed intervals in the sense of Ghibaudo,
122 1992). The thickness, grain size, presence of erosion surfaces, mud clasts and structure of every
123 internal division of the beds were recorded separately for each bed in addition to the total bed
124 thickness. The grain size was measured using a grain-size comparator chart. In order to account for
125 amalgamation of beds, partially amalgamated beds were measured as individual layers. This was
126 possible through detecting the subtle grain-size breaks that are associated with amalgamation surfaces.
127 To make the measure of the section reproducible and available also for other analyses labeled nails
128 were fixed every metre from the base to the top of the section, according to the attitude of the bedding.

129

130 **Body fossils**

131 Fossils were collected bed by bed, from a total of 144 beds over the whole studied section; for each of
132 the targeted beds, two rectangles (50 cm wide and 10 cm tall) were delimited and all fossil exposed
133 sampled. Fossil specimens (mainly molluscs) were then washed and cleaned from the encasing
134 sediment using an air drill, in case of hard sediment, or a scalpel, in case of soft sediment, and a unique
135 ID was assigned to each of them; they were identified at generic and/or specific level (where feasible)
136 based on relevant literature (e.g., Ceregato et al., 2007; Williams et al., 2000, 2006; Crippa and Raineri,
137 2015) and subsequently counted (see Appendix A1 in the Supplementary information online for a
138 detailed explanation). In addition, to aid environmental interpretation of fossil assemblages, it was
139 observed if the specimens (bivalves and brachiopods) were articulated or disarticulated and each
140 specimen retrieved was carefully inspected looking for the presence of the following taphonomic
141 features: a) roundness vs sharpness of fragments; b) corrosion, due to the combined effect of abrasion

142 and dissolution (Brett and Baird, 1986); c) external and/or internal bioerosion, produced by predators,
143 necrophages or by the presence of domichnia; d) internal and/or external encrustations, caused by
144 episkeletobionts (sensu Taylor and Wilson, 2003); e) ornamentation, which is usually fragile and can
145 be lost during post-mortem processes and f) original color and pattern of the shell/fragment surface (see
146 Appendix A2 and Table A1 in the Supplementary information online). Based on the analysis of these
147 features, we identified the associations defined by Brenchley and Harper (1998): 1) life assemblages, 2)
148 neighborhood assemblages and 3) transported assemblages.

149 A qualitative palaeoecological analysis was then performed, where the assemblages of the Arda River
150 section have been tentatively compared to the recent Mediterranean biocoenoses. As the majority of the
151 retrieved taxa is represented by living species, the fossil associations recovered were grouped in
152 biofacies and attributed to the present day depositional environments based on the occurrence of
153 characteristic taxa described by Pérès and Picard (1964). The abbreviations used are: SFBC: biocoenosis
154 of fine-grained well sorted sands; SFS: biocoenosis of shallow water fine-grained sands; DC:
155 biocoenosis of coastal detritic bottoms; VTC: biocoenosis of terrigenous mud.

156

157 **Trace fossils**

158 Sedimentology and body fossil palaeontology have been integrated with ichnological analysis, using
159 the workflow for integrated facies analysis (McIlroy, 2008). Because of the predominantly vertical
160 outcrops and the high bioturbation intensity, the ichnofabric approach has been used. The ichnofabric
161 analysis method considers the overall texture of a bioturbated sediment and as such it is the
162 ichnological equivalent of facies analysis (Taylor et al., 2003; McIlroy, 2004, 2008).

163 Data collection consisted of recording the ichnofabric attributes of the Arda River section in the field at
164 regularly spaced intervals ('samples'). Each of the studied samples was approximately 25 cm thick and
165 the spacing between successive samples was 1 m. The recorded ichnofabric attributes are: 1) primary

166 sedimentology (Taylor et al., 2003), 2) degree of bioturbation, quantified by the ichnofabric index (ii)
167 methodology (Bottjer and Droser, 1991), 3) components of the ichnofabric, including either distinct
168 trace fossils or biodeformational structures with indistinct outlines (Schäfer 1956; Wetzel and Uchman,
169 1998; Taylor et al., 2003). Relative abundance, burrow size, tiering, trace fossil frequency and
170 distribution at the sample scale have also been observed (Bromley, 1996; Taylor et al., 2003; Gingras et
171 al., 2011).

172 Visual analysis of each sample included observation of 1) the weathered surface of the outcrop; 2) the
173 fresh surface of the outcrop, exposed with a trowel; a minimum of three fresh surfaces of about 25x25
174 cm have been observed and 3) the enhanced fresh surface, obtained by dropping water on the fresh
175 surface to enhance colour contrast and to differentiate weathered traces from the surrounding sediment.
176 Each sample has been attributed to an ichnofabric class that has been distinguished on the basis of the
177 degree of bioturbation, bioturbation distribution (Gingras et al., 2011), diversity (i.e., the number of
178 ichnotaxa present; Bromley, 1996) and components of the ichnofabric.

179

180 **RESULTS AND INTERPRETATIONS**

181 **Facies analysis**

182 Facies analysis was carried out in marine sediments deposited during phases of advance of fan deltas
183 when Apennine tectonic uplift renewed sediment dispersal and provided the basin with a steeper
184 margin. Following the genetic classification scheme proposed by Zavala et al. (2011) for flood-
185 generated delta-front lobes, the deposits of the Arda section (Fig. 2) have been grouped in three main
186 facies categories related to the three main processes that characterise sustained hyperpycnal discharges
187 (i.e., *hyperpycnal flows*; Mutti et al., 2000; Tinterri, 2007) in marine settings: 1) *bed load* (Facies B:
188 bed-load related sedimentary facies), 2) *turbulent suspension* (Facies S: suspended-load-related

189 sedimentary facies), and 3) *lofting* (Facies L: lofting-related sedimentary facies). Facies code and
190 relative description are shown in Table 1.

191 *Facies related to bed-load processes (Facies category B)*

192 Facies category B is composed of massive (GmE; Fig. 3 A) and cross-stratified (or crudely stratified)
193 conglomerates (Gp; Fig. 3 D) with abundant coarse- to fine-grained sandstone matrix (matrix
194 supported). Large clasts in this facies appear to float in a medium- to coarse-grained sandstone matrix.
195 Individual sets of crossbedding commonly show thicknesses between 0.1 and 0.5 m. The foreset
196 inclination in general does not exceed 15°. Bounding surfaces between bedsets can be erosional. Lag
197 deposits (Lag; Fig. 3 E, F) represented by gravel carpets with bioclastic and sandy (very coarse) matrix
198 are frequent. This facies category also includes mud clast-supported conglomerate (GmM; clay-chips;
199 Fig. 3 A, B, C). Mudstone intraclast diameter ranges from 0.5 up to 20 cm and their shapes range
200 accordingly from rounded sub-spherical to rounded tabular.

201 Interpretation: this facies category includes different coarse-grained deposits related to shear/drag
202 forces exerted by the overpassing long-lived turbulent (hyperpycnal) flow over coarse-grained
203 materials lying on the flow bottom (Fig. 3). High-density flows triggered by river floods can mix and
204 deposit skeletal remains from different shallow-water communities. Regardless, accumulations of
205 shells are rare features in this bed-load related sedimentary facies.

206 *Facies related to the collapse of suspended load (facies category S)*

207 Facies category S (Fig. 4) are mostly fine-grained sandstone strata ranging from a few millimetres thick
208 lamina-sets, to several tens of decimetres thick beds and bedsets, with massive stratification (Sm; Fig. 3
209 E, F), horizontal (Sh; Fig. 4 A, D) or hummocky cross stratification (HCS; Fig. 4 E), tabular and
210 oblique cross stratification (Sp, Sx; Fig. 4 B), and small-scale cross lamination (Sr, St; Fig. 4 A, C).
211 Many beds are sharp based and fine upward, with structures ranging from horizontal or large-scale
212 wavy lamination to small scale cross lamination (wavy, sigmoidal, and/or climbing ripple structures).

213 Small floating clay chips are common and are dispersed within the sandstone body or grouped toward
214 the top.

215 Accumulations of shells are common features in the sandstone intervals, where they form thick, sharp-
216 based, sometimes normally graded lags at the base of massive (Sm; Fig. 3 E. F) or laminated strata (Sp,
217 Sx, Sr; Fig. 4 A, B. C). Shell-bed geometry ranges from tabular to lenticular; shells are always closely
218 packed, mostly concave-down, and sometimes imbricated. In many cases, tabular, sharp-based shell
219 beds (that are 10–50 cm thick and broadly lenticular) are found at the base of horizontal or hummocky
220 cross-stratified (HCS) beds. Carbonaceous remains and wood fragments (commonly leaves with
221 exceptional preservation) are also common within massive sands. Sedimentary structures are rarely
222 disrupted by bioturbation, but bedtops may be 100% bioturbated. Flasers and massive mudstone beds
223 (HeB), from a few millimetres to several centimetres thick, are often intercalated with the sandstones.
224 Interpretation: this facies is mostly composed of fine-grained sediments transported as suspended load,
225 forming thick and commonly complex intervals that can be massive or display traction plus fallout
226 sedimentary structures.

227 *Facies related to flow lofting (facies category L)*

228 Facies category L (Fig. 5) is characterised by thin couplets of massive to laminated siltstones and
229 mudstones (Fm; Fig. 5 A). The individual levels commonly display a variable thickness from a few
230 millimetres up to 100 cm. Marine bivalves in life position are present in the lower part of the
231 stratigraphic section.

232 Interpretation: this facies is composed of the finest materials transported by the hyperpycnal flow,
233 which accumulated by normal settling when the flow completely stopped.

234 *Facies association*

235 On the basis of high-resolution stratigraphic framework, the marine sedimentary succession up to 217
236 m is characterised by at least six (labeled I–VI in Fig. 2), 5–25 m-thick fining upward cycles deposited

237 by high-density turbidite flows (hyperpycnal flow, *sensu* Mutti et al., 2000) that grade into hemipelagic
238 siltstones and mudstones (Fig. 2). These cycles are often very complex, showing internal erosional
239 surfaces and gradual facies recurrences.

240 Each cycle usually starts with massive to cross-bedded conglomerates (GmE, GmM, Gp, Lag; Table 1)
241 with abundant bioclastic and sandy matrix. Intraclasts and accumulations of shallow-water skeletal
242 remains are also present. Bedset-bounding surfaces can be erosional (Fig. 5 C). Above follow
243 sandstones that are either massive or with horizontal, hummocky, tabular or oblique cross stratification
244 (Sp, Sx, HCS, St, Sr, Sh, Sm; Table 1). Sharp based, normally graded, tabular to lenticular lags of
245 concave-down shells may occur at the base of the strata. Carbonaceous remains and wood fragments
246 are also common within massive sands. Flasers, wavy and lenticular bedding (Heb; Table 1), from a
247 few mm- to several cm-thick, are often intercalated with these sandstones. Finally, above the
248 sandstones follow massive to laminated siltstones and mudstones arranged in thin couplets (Fm; Table
249 1), ranging in thickness from a few mm up to 1 m and accumulated by normal settling when the flow
250 completely stopped.

251 Each cycle shows a complicated internal arrangement. The vertical and lateral facies anisotropy and the
252 relatively rapid accumulation result in the common occurrence of water-escape features such as load
253 cast and flame structures (Fig. 5 D). Field observations suggest a close association of this facies with
254 channel fill deposits.

255 At 45 m from the base of the succession a biocalcarenite body occurs (Fig. 5 E, F). It forms basinward-
256 prograding wedges composed of alternating well or poorly cemented layers with dense accumulations
257 of reworked shells. It typically displays a tripartite geometry, whose topset horizontal strata are
258 intensely bioturbated, and may contain abundant articulated bivalves and fragmented calcareous algae,
259 whilst foresets and bottomsets are characterised by dense accumulations of reworked shells.

260 From 130 to 132 m, very fine-grained limestones form lenticular or pinching and swelling beds, up to
261 0.25 m thick (Fig. 5 B). The beds have sharp bases and tops and may be laminated. The thin section
262 analysis reveals that these beds are predominately composed of a fine-grained calcareous matrix
263 including calcareous microspheroids and organic matter.

264 From 217 to 237 m, the sequence is characterised by coarse-grained sands and pebbly sandstones with
265 low-angle cross-stratification (Sx, Sh, St, Sm, HCS, Heb; Table 1). Large clasts appear floating in a
266 medium- to coarse-grained sandstone matrix. Individual sets of cross-beds (Sx, St) commonly show
267 thicknesses between 0.3 and 1 m and asymptotic relationships with top and base. The foreset
268 inclinations do not usually exceed 20°. This facies association is attributed to littoral (transitional)
269 environments.

270 From 237 to 300 m, the sequence comprises continental sediments arranged in four main cycles, each
271 characterised by massive or crudely stratified, partially cemented, fluvial gravel beds (from 1 m to 4 m-
272 thick; GmE, Gp; Fig. 2, Table 1), passing rapidly upward to sands, silts and muds packed in beds from
273 few metres up to 15 m thick. In situ root systems and tree trunks, together with CaCO₃ nodules and
274 typical terrestrial gastropods [e.g., *Pomatias elegans*, *Carychium tridentatum*, *Retinella (Retinella)*
275 *olivetorum*] are abundant in fine grained beds, suggesting continental swamp environments.

276 Interpretation: Deposits of the Arda section display a complicated vertical arrangement of different
277 lithofacies reflecting cyclic depositional changes between suspended-load and bed-load-dominated
278 facies associated with different velocity and fallout rates. These cyclical and gradual changes between
279 different facies are the result of near-continuous deposition from a quasi-steady turbulent flow (Zavala
280 et al., 2011). Distinctive features observed in the studied deposits are: i) the sharp based and normally
281 graded beds containing HCS, ii) gradual and sharp facies transitions without a definite and predictable
282 internal arrangement, iii) the abundant rip-up mudstone clasts and shells, iv) internal and laterally
283 discontinuous erosional surfaces, v) scarce burrows, and vi) a basal coarsening-upward interval (Mutti

284 et al., 2000; Zavala et al., 2006, 2011). The studied deposits evolve laterally into packages of lofting
285 rhythmities. These features are most likely related to bed-load processes developed at the base of a
286 hyperpycnal flow (i.e., long-lived turbulent flow) and tend to dominate the proximal to medial parts of
287 a river-delta system.

288 The biocalcarenite body occurring at 45 m from the base of the succession shows an internal geometry
289 suggesting that biocalcarenitic deposits are formed during periods of decreased input of fine-grained
290 terrigenous sediments (or sediment starved conditions) whose fossiliferous content indicates high-
291 energy levels in the shelf environments. Different physical conditions can be assumed for their
292 formation such as reduced terrigenous input or strong bottom reworking by currents. Massari and
293 Chiocci (2006) describe the formation of very similar Pliocene-Quaternary basinward-prograding
294 biocalcarenite wedges (detached from the shore and below the storm-wave base) along the submerged
295 margins of the Mediterranean area by means of processes of sediment reworking from a nearshore by
296 pass zone and of storm-driven down-welling flow. The cyclical nature of these biocalcarenites,
297 observed in the Castell'Arquato basin (Stirone section, Cau et al., 2013, 2017), has been hypothesised
298 to be orbitally-controlled by obliquity and/or precession cyclicity.

299 According to Mutti et al. (2003), the Arda River succession can be interpreted as a flood-dominated
300 fan-delta system accumulated in roughly tabular lobes extending from alluvial conglomerates to shelfal
301 siltstone and mudstone. The associate deposits (hyperpycnites; Mulder et al., 2003) are closely related
302 to direct fluvial discharge. Observed facies associations clearly show as flood-generated dense flows
303 enter seawaters as catastrophic and inertia-dominated relatively unconfined flows. Coarser materials
304 tend to accumulate at the front of the flow, giving way to a horizontally negative grain-size gradient.
305 Sedimentation occurs mainly in a mouth bar (characterised by sigmoidal bedding) and in associated
306 flood-generated delta-front sandstone lobes.

307 This study suggests that the Arda River succession corresponds to the subaqueous extension of a fluvial
308 system. It originated when the river in flood directly discharged a sustained (Carruba et al., 2004;
309 Felletti et al., 2009) and relatively denser turbulent mixture of fresh water and sediments (hyperpycnal
310 flows; Bates, 1953) into the receiving standing body of water. This system extended for kilometres
311 away from the river mouth and developed a predictable path of genetically related facies (Browne and
312 Naish, 2003; Mancini et al., 2013; Marini et al., 2013; Milli et al., 2016; Bruno et al., 2017) during its
313 travel basinward.

314

315 **Body Fossils**

316 The fossil associations of the Arda River succession contain a very diversified fauna composed mainly
317 of several species of bivalves and gastropods; brachiopods, corals, serpulids, echinoderms, scaphopods
318 and barnacles do also occur. The associations have been grouped into 11 biofacies, based on the
319 presence of key species, taphonomic evaluation (A2 and Table A1 in the Supplementary information
320 online) and (palaeo)ecology of the fossils recovered (Figs. 6 A-F, 7 A-F; 8.1-14).

321 *Biofacies 1*

322 This biofacies occurs in fine-grained massive siltstones and sandstones (Facies L) at the base of the
323 section (37.05-43.25 m). It is composed mainly of seminafaunal/infaunal organisms and by
324 cemented/byssate epifaunal taxa; many rheophilous taxa (e.g., *Astarte fusca*, *Glycymeris inflata*,
325 *Glycymeris glycymeris*, *Clausinella fasciata*) are present (Figs. 6 A; 8.1, 3, 4). The taphonomic
326 preservation is generally good (A2 and Table A1 in the Supplementary information online).

327 Interpretation: The occurrence of disarticulated rheophilous shelf related taxa indicates neighborhood
328 assemblages of a high-energy environment winnowed by currents in an offshore transition setting. The
329 negligible presence of shoreface key taxa (*Chamelea gallina*, *Spisula subtruncata* and *Acanthocardia*
330 *tuberculata*) showing high taphonomic degradation suggests a transport from shallower settings.

331 *Biofacies 2*

332 This biofacies occurs in fine-grained massive silty to muddy lithologies (Facies L) below and above the
333 biocalcarenitic body (44.90 m; 47.35-49 m; 56.35-58.35 m); it is mainly represented by few specimens
334 of seminafaunal/infaunal species typical of muddy-detritic and muddy shelf substrates (e.g., *Venus nux*,
335 *Turritella tricarinata pliorecens*, *Naticarius stercusmuscarum*, *Pelecypora brocchii*), showing an
336 excellent preservation (Fig. 6 C, D. A2 and Table A1 in the Supplementary information online). Corals,
337 echinoids, brachiopods and non-rheophilous molluscs are also present.

338 Interpretation: The sparse presence of *V. nux* and *P. brocchii* along with echinoids, brachiopods and
339 corals suggest a low-energy lower offshore transition setting, characterised by normal marine salinity
340 and oxygen conditions

341 *Biofacies 3*

342 This biofacies occurs in biocalcarenite (45.65-46.05 m; Facies S) and is represented by sparse and
343 poorly preserved valves of epifaunal molluscs: *Aequipecten opercularis*, *Aequipecten scabrella* and
344 *Ostrea edulis* (A2 and Table A1 in the Supplementary information online).

345 Interpretation: The sparse mollusc content associated with poor taphonomic preservation within coarse-
346 grained deposits allows only a generic interpretation of a transported assemblage from relatively high-
347 energy settings.

348 *Biofacies 4*

349 This biofacies occurs in fine-grained massive siltstones (59-70.02 m; 106.50-111.60 m; Facies L).
350 Several key infaunal shoreface to offshore transition well preserved taxa typical of muddy sands are
351 found, specifically *Glycymeris insubrica*, *A. tuberculata*, *C. gallina*, *S. subtruncata*, *Neverita*
352 *josephinia* (Figs. 6 E; 8.5, 6; A2 and Table A1 in the Supplementary information online).

353 Interpretation: The ecological and taphonomic signatures of this biofacies suggest life and
354 neighborhood assemblages of shallow marine, high-energy offshore transition environments (Facies L);

355 the faunal composition can be compared to the recent Mediterranean biocoenosis of SFBC (Pérès and
356 Picard, 1964).

357 *Biofacies 5*

358 This biofacies occurs in an alternation of fine-grained sandy to silty and muddy lithologies (217.90-
359 223.20 m; 230.80-237 m; Facies S and B). It contains mainly seminafaunal/infaunal taxa living in
360 shallow water muddy sands (e.g., *G. insubrica*, *A. tuberculata*, *C. gallina*, *Ensis ensis*, *Loripes*
361 *orbiculatus*, *Cylichna cylindracea*, *Atlantella pulchella*, *N. josephinia*), together with species of upper
362 shoreface (*Donax* spp.) and of wave-protected environments (*Lucinella divaricata*) (Figs. 7 C-F; 8.12).
363 Toward the top, *G. insubrica* becomes the most abundant species (Fig. 7 E, F), with numerous
364 articulated specimens found in life position in muddy beds; trunks and plant remains are also found. All
365 the specimens are well preserved (A2 and Table A1 in the Supplementary information online).

366 Interpretation: Biofacies 5 indicates life and neighborhood assemblages of upper shoreface setting, due
367 to the presence of key taxa *Ensis ensis* and *Donax* spp.; the faunal composition is comparable to the
368 SFBC and SFS biocoenoses of the recent Mediterranean Sea (Pérès and Picard, 1964).

369 Seminafaunal/infaunal taxa are dominant, suggesting a high-energy shallow water environment, which
370 may prevent the colonization by epifaunal species; however, the presence of species living in wave-
371 protected environments suggests a more heterogeneous substrate with quieter areas. Also, toward the
372 top of the section, the disappearance of stenohaline species and the increase of euryhaline taxa,
373 suggests settings affected by river discharge. Indeed, *G. insubrica*, which can also thrive in low salinity
374 settings (e.g., Malatesta, 1974; Raineri, 2007; Crnčević et al., 2013) becomes the dominant species in
375 this upper part. Biofacies 5 differs from Biofacies 4 by the presence of shallower water taxa (e.g.,
376 *Donax* spp.), which are absent in Biofacies 4.

377 *Biofacies 6*

378 This biofacies is found in fine-grained massive clayey horizon (224.20-224.30 m; Facies L), hosting
379 several articulated specimens of *Arctica islandica* in life position and lacking sediment filling inside the
380 valves (Fig. 7 B), associated to the shallow water *S. subtruncata*, (average preferred depth: 6.60 m,
381 standard deviation: 7.3 m; Wittmer et al., 2014) both showing an excellent preservation (A2 and Table
382 A1 in the Supplementary information online).

383 Interpretation: The co-occurrence of lower shoreface *S. subtruncata* and of the “northern guest” *A.*
384 *islandica* suggests a lower shoreface/offshore transition setting.

385 *Biofacies 7*

386 This biofacies occurs in fine-grained massive silts and clays (Facies L) (146.55-167.90 m, 196-207 m).
387 Seminafaunal/infaunal taxa living in muddy to silty lithologies are dominant. *V. nux* is the most
388 abundant species in this interval, together with *Turritella tricarinata pliorecens*, *Glossus humanus*,
389 *Aporrhais pespelecani*, *Acanthocardia paucicostata* and *Saccella commutata*, all showing an excellent
390 preservation (Fig. 8.2, 8; A2 and Table A1 in the Supplementary information online).

391 Interpretation: The abundance of *V. nux* suggests a low-energy offshore transition setting which can be
392 compared to the recent VTC biocoenosis of the Mediterranean Sea (Pérès and Picard, 1964). According
393 to Taviani et al. (1997) and Dominici (2001) the *Venus nux* assemblage lived at water depths of 20–40
394 m.

395 *Biofacies 8*

396 This biofacies (80.30-91.40 m; 101-104.10 m; 122.90-125.50 m; Facies L) comprises well preserved
397 epifaunal species of mainly muddy/sandy-detritic settings (e.g., *Pecten jacobaeus*, *Aequipecten*
398 *opercularis*, *Flexopecten flexuosus*, *Pitar rudis*), occurring together with mud-loving infaunal species
399 (as *V. nux* and *T. tricarinata pliorecens*) where the mud content increases (A2 and Table A1 in the
400 Supplementary information online).

401 Interpretation: This biofacies is characterised by many key species (e.g., *P. rudis*, *F. flexuosus*, *P.*
402 *jacobaeus*) belonging nowadays to the recent DC biocoenosis (Pérès and Picard, 1964) together with
403 VTC species where the mud content increases, all indicating life or neighborhood assemblages of
404 offshore transition environments.

405 *Biofacies 9*

406 This biofacies is found in an alternation of fossil rich fine-grained sands/silts and mud barren of fossils
407 (127.95-146.45 m; Facies S and B). The fauna consists of well preserved seminafaunal/infaunal species
408 together with few epifaunal ones; taxa of shallow water muddy sands are abundant (e.g., *G. insubrica*,
409 *C. gallina*, *A. tuberculata*, *E. ensis*, *Tritia mutabilis*) together with few sandy/muddy-detritic species
410 (*A. opercularis*, *Laevicardium oblongum*, *P. rudis*) (Figs. 6 F, 7 A; 8.7; A2 and Table A1 in the
411 Supplementary information online). Occasionally *Ditrupa* sp. horizons are retrieved (e.g., ACG95;
412 Table A1 in the Supplementary information online).

413 Interpretation: This biofacies suggests neighborhood assemblages of shoreface settings, which thank to
414 the presence of *G. insubrica*, *C. gallina*, *A. tuberculata*, *E. ensis* and *T. mutabilis* can be compared to
415 SFBC biocoenosis of the recent Mediterranean Sea (Pérès and Picard, 1964), although few DC taxa
416 (e.g., *L. oblongum*, *P. rudis*) are also found. Biofacies 9 is similar to Biofacies 5, although very shallow
417 water taxa have not been identified here. The occasional presence of monotaxic beds of *Ditrupa* sp.,
418 usually thriving in turbid waters conditions (Dominici, 2001), suggests unstable and loose substrates.

419 *Biofacies 10*

420 This biofacies occurs in several sandstones beds of the succession within Facies S and B (54-54.20 m;
421 92.50-98.30 m; 170-194.10 m; 208.40-210.40 m) and is characterised by containing ecologically mixed
422 and generally poorly preserved taxa (Fig. 8.9-11, 13, 14; A2 and Table A1 in the Supplementary
423 information online), often associated to clay chips and vegetal debris; an exception is given by well
424 preserved, articulated specimens of *Pinna* sp. and infaunal echinoids. Seminafaunal/infaunal and

425 epifaunal species of shelf muddy/sandy-detritic settings (e.g., *L. oblongum*, *Timoclea ovata*, *P. rudis*, *P.*
426 *jacobaeus*) are associated to shallower water species (e.g., *A. pulchella*, *C. gallina*, *G. insubrica*, *S.*
427 *subtruncata*) and mud loving taxa (e.g., *Nucula placentina*, *T. tricarinata pliorecens*, *V. nux*).

428 Interpretation: This biofacies, characterised by an ecologically mixed poorly preserved fauna of
429 shoreface to offshore transition settings, represents mainly transported assemblages finally buried in an
430 offshore transition setting as testified by articulated *Pinna* sp. and infaunal echinoids in life position
431 (Fig. 6 B); this suggests a high-energy setting as indicated also by the facies analysis (Facies S and B).

432 *Biofacies 11*

433 This biofacies groups species poorly preserved and ecologically mixed (e.g., *A. tuberculata*, *A.*
434 *opercularis*, *V. nux*) found within conglomerate beds (217.20 m; 223.80 m; Facies B; A2 and Table A1
435 in the Supplementary information online).

436 Interpretation: The high taphonomic degradation along the different ecology of the species recovered
437 reflects transport/reworking in a high-energy, coarse-grained shallow marine settings.

438

439 **Trace Fossils**

440 The samples of the Arda River section have been attributed to 15 ichnofabric classes, that are grouped
441 in 4 ichnofabric groups based on bioturbation intensity, distribution and diversity (Table 2). Ichnofabric
442 groups have been named according to the dominant feature, and ichnofabric classes have been named
443 according to the dominant traces. Ichnotaxa have been identified at the ichnogenus level and open
444 nomenclature has been used for difficultly identifiable traces. Readers are addressed to Table A2 in the
445 Supplementary information online for details on ichnotaxa.

446 *Ichnofabric group 1 - low-moderate bioturbation, homogeneous distribution of traces, low*
447 *diversity*

448 The ichnofabric classes of group 1 typically present low to moderate bioturbation intensity,
449 homogeneous distribution of traces at the scale of the sampling unit and low diversity of traces:

450 (1) Unbioturbated ichnofabric. Unbioturbated conglomerates (Facies GmE, Gp);

451 (2) Low bioturbation ichnofabric. Unbioturbated or sparsely bioturbated (ii 1-2) sands with
452 monogeneric assemblages of *Planolites*, *Palaeophycus*. Cryptobioturbation locally present;

453 (3) *Skolithos* ichnofabric. *Skolithos* occurring in massive sands (Facies Sm);

454 (4) *Ophiomorpha* ichnofabric (Fig. 9 A-C). *Ophiomorpha* preserved as full-reliefs in planar- or
455 cross-laminated sands (Facies Sh);

456 (5) *Macaronichnus* ichnofabric (Fig. 9 D-F). *Macaronichnus* preserved in faintly laminated
457 sands with rare shell debris (Facies Sm).

458 Interpretation: The low to moderate bioturbation intensity is interpreted as the result of a stress factor
459 that prevented total bioturbation of the sediment (Bromley, 1996; Taylor et al., 2003). The
460 homogeneous distribution of traces indicates that the stress factors were persistent, at least at the scale
461 of the observation unit (Gingras et al., 2011). Specifically, the ichnofabric classes are interpreted as
462 follows:

463 (1) Unbioturbated ichnofabric. The lack of bioturbation suggests the original lack of
464 endobenthic activity or the non-preservation of biogenic structures (Bromley, 1996). Because this
465 ichnofabric is characterised by bed load related facies, it is likely that physical stress, represented by
466 high hydrodynamics and shifting substrates, prevented endobenthic colonization of these units.

467 (2) Low bioturbation ichnofabric. This ichnofabric reflects the work of trophic generalists (the
468 producers of *Planolites* and *Palaeophycus*; see Gingras et al., 2011). Brackish setting is suggested by
469 low ichnodiversity, simple structures produced by trophic generalists, monospecific associations and
470 small size (Pemberton et al., 2001; Buatois et al., 2005; Hauck et al., 2009; Buatois and Mángano,
471 2011). These features are consistent with a foreshore to middle shoreface environment.

472 (3) *Skolithos* ichnofabric. Based on the distribution of both animal and plant *Skolithos*
473 (Bromley, 1996; Gregory et al., 2006; Knaust, 2017), this ichnofabric is interpreted to reflect marine
474 (foreshore to upper shoreface) or, at least, marine-influenced (backshore) settings. A more precise
475 environmental interpretation of this ichnofabric is difficult, also because plant ichnology is an
476 understudied field (Baucon et al., 2012).

477 (4) *Ophiomorpha* ichnofabric. This ichnofabric represents the work of a deep-tier community of
478 trophic generalists (the producers of *Ophiomorpha*). The constructional lining of *Ophiomorpha* is a
479 strategy to cope with high-energy and shifting substrates (Frey et al., 1978; Coelho and Rodrigues,
480 2001; Pemberton et al., 2001; Taylor et al., 2003; Buatois and Mángano, 2011; Gingras et al., 2011).
481 These features are consistent with a high-energy foreshore to shoreface environments (see Pemberton
482 et al., 2001; Baucon et al., 2014; Leaman et al., 2015). Based on the palaeoclimatic significance of
483 *Ophiomorpha* (Goldring et al., 2004, 2007), this ichnofabric is regarded as a warm water indicator.

484 (5) *Macaronichnus* ichnofabric. This ichnofabric represents the work of a deep-tier community
485 of selective deposit feeders, well-adapted to soft substrates with very high hydrodynamics at the water-
486 sediment interface. These environmental parameters are compatible to foreshores and shorefaces, as
487 also suggested by the environmental preferences of *Macaronichnus* (high-energy foreshores and
488 shallow shorefaces: Clifton and Thompson, 1978; Pemberton et al., 2001; Savrda and Uddin, 2005;
489 Seike et al., 2011; Pearson et al., 2013). *Macaronichnus* has been proposed as an indicator of temperate
490 to cold waters (Quiroz et al., 2010).

491 *Ichnofabric group 2 - low-moderate bioturbation, heterogeneous distribution of traces, moderate*
492 *diversity*

493 The ichnofabric classes of group 2 are characterized by regular heterogeneous distribution of traces.
494 Traces are preserved in heterolithic facies (Fig. 10 A) consisting of alternating sand and mud layers
495 (Facies HeB). Mud layers commonly present biogenic structures with poorly defined wall (e.g.,

496 *Planolites* and mantle and swirl structures) (homogeneous suite; Fig. 10 B) and “sharp walled burrows”
497 (sharp burrows suite; Fig. 10 C-E). Sand layers are typically bioturbated by lined burrows (e.g.,
498 morphotype A of *Schaubcylindrichnus?*; Fig. 10 F) and/or smooth-walled traces (e.g., *Scolicia*; Fig. 10
499 G, H). This ichnofabric group comprises three ichnofabric classes, distinguished on the basis of the
500 paucity of “sharp walled burrows” (few sharp burrows – smooth burrows ichnofabric), the dominance
501 of scoliceids (Sharp burrows – Scoliceids ichnofabric) and the abundance of “sharp walled burrows”
502 (Sharp burrows – smooth burrows ichnofabric).

503 Interpretation: The regular heterogeneous distribution of trace fossils indicates regular variability in the
504 physico-chemical conditions and iterative colonization events (Gingras et al., 2011). Based on the idea
505 that burrow boundary stores information about the sediment consistency (Uchman and Wetzel, 2011),
506 these events are interpreted as follows:

507 (1) Colonization of soupground to softground mud. Traces of the homogeneous suite represent
508 the work of organisms ‘swimming’ in soupgrounds (mantle and swirl traces) or deposit-feeding in
509 firmer substrates (*Planolites*) (Lobza and Schieber, 1999). Settling of hypopycnal plumes or lofting of
510 hyperpycnal flows are interpreted to be the major depositional processes because of sedimentological
511 evidences and the ichnological similarity with other hyperpycnites (Bhattacharya and MacEachern,
512 2009);

513 (2) Dewatering and colonization of firmground mud. The unlined, passively filled burrows of
514 the sharp burrows suite suggest that the sediment became firm enough to avoid collapse of unlined
515 burrows themselves (see Uchman and Wetzel, 2011; Fürsich, 1978; Bromley, 1996);

516 (3) Erosion and event deposition. The passive fill of the sharp burrows suite suggests that, after
517 colonization of firmground muds, an abrupt depositional event brought sand to the seafloor.
518 Hyperpycnal flowing is interpreted to be the major depositional process (see Bhattacharya and
519 MacEachern, 2009).

520 (4) Colonization of looseground sand. The smooth burrows suite represents the community that
521 colonized sand brought to the seafloor by event deposits ('post-depositional suite'; Książkiewicz, 1954;
522 Seilacher, 1962; Uchman and Wetzel 2011). Lining indicates that the substrate was soft and
523 unconsolidated (Bromley, 1996).

524 For these reasons, the ichnofabric classes of this group are interpreted to reflect bioturbation of muddy
525 seafloors during low-energy conditions and colonization of sandy event (hyperpycnal) deposits. Based
526 on bioturbation intensity, ichnodiversity and tiering complexity, the ichnofabric classes of this group
527 are interpreted to reflect a stress gradient, including persistently stressed marine environments (few
528 sharp burrows – smooth burrows ichnofabric), temporarily stressed environments (sharp burrows-
529 scollicids ichnofabric) and stable environments (sharp burrows – smooth burrows ichnofabric).

530 According to the palaeoclimatic significance of *Scolicia* (Goldring et al., 2004, 2007), the sharp
531 burrows-scollicids ichnofabric is interpreted to represent temperate to warm waters. It should be also
532 noted that *Scolicia* is associated to normal marine salinity (Buatois and Mángano, 2011), well-
533 oxygenated porewaters (Löwemark et al., 2006; de Gibert and Goldring, 2008; Uchman and Wetzel,
534 2011), restricted competition by organisms of deeper-burrowing tiers (Fu and Werner, 2000), at times
535 being correlated with bottom currents and high sedimentation rates (Fu and Werner, 2000; Löwemark
536 et al., 2006; Wetzel et al., 2011).

537 *Ichnofabric group 3 - moderate-high bioturbation, homogeneous distribution of traces, low*
538 *diversity*

539 Ichnofabric group 3 includes a very heterogeneous set of ichnofabric classes with sharp-walled traces
540 and/or passively filled burrows:

541 (1) *Lockeia* ichnofabric (Fig. 11 A, B). Cemented carbonatic beds (Facies CCB) with no distinct
542 burrows, or predominantly monogeneric (e.g., *Lockeia*, *Ophiomorpha*, *Diplocraterion*) assemblages;

543 (2) *Thalassinoides* ichnofabric (Fig. 11 C, D). Horizontal *Thalassinoides* bioturbating
544 plurimetrical layers of bioclastic sands (Facies Sp). “Y-shaped burrows” and bioerosion structures on
545 shells (e.g., *Entobia*) are also present;

546 (3) Coarse-fill burrows ichnofabric (Fig. 11 E). Irregular mottles and circular sharp-walled
547 burrows (*Thalassinoides*?) filled with coarse-grained sand or fine-grained conglomerate.

548 Interpretation: Low diversity and homogeneous distribution of traces suggest persistently stressed
549 conditions or preservation of elite trace fossils by upward migration of deep tiers (Bromley, 1996):

550 (1) *Lockeia* ichnofabric. Cementation is a post colonization feature for the *Ophiomorpha*-
551 dominated assemblages because a loose substrate is required by its tracemakers to manipulate the
552 characteristic pellets of the burrow lining. Other assemblages show some of the characteristics of the
553 substrate-controlled *Glossifungites* ichnofacies (i.e., presence of sharp-walled, unlined dwelling
554 burrows of suspension feeders; dominance of robust, vertical to subvertical, simple and spreite U-
555 shaped burrows; low ichnodiversity; high abundance; Buatois and Mángano, 2011). They could
556 represent substrates that became stiff before of the colonization by shallow-tier suspension-feeding
557 organisms. Presence of food in suspension and lack of deep-tier deposit feeders suggests an energetic
558 environment, possibly a high-energy foreshore.

559 (2) *Thalassinoides* ichnofabric. This ichnofabric occurs in plurimetrical units bioturbated by
560 *Thalassinoides*, implying that it results from the upward migration of a deep-tier. This feature and the
561 passive bioclastic fill suggests that this ichnofabric is the result of repeated cycles of colonization,
562 passive infilling and deposition. The tubular tempestite model, consisting of the repetitive excavation
563 and storm infilling of burrow networks, could explain this pattern (Tedesco and Wanless, 1991).

564 (3) Coarse-fill burrows ichnofabric. Sharp wall and passive fill indicate that biogenic structures
565 have been emplaced in firmground muds and maintained as open burrows (Buatois and Mángano,
566 2011; MacEachern et al., 2007, 2012). Because the burrow fill differs from surrounding and overlying

567 sediments, this ichnofabric class represents a trace-fossil omission suite that preserves a high-energy
568 event that would otherwise have passed unnoticed (see MacEachern et al., 2012). These features are
569 consistent with an environment dominated by sediment bypass, such as the margins of a submarine
570 canyon, that is a typical depositional setting of the *Glossifungites* ichnofacies (Buatois and Mángano,
571 2011).

572 *Ichnofabric group 4 - high bioturbation, homogeneous distribution of traces, moderate to high*
573 *diversity*

574 The ichnofabric classes of group 4 are typically characterized by intense bioturbation:

575 (1) Scolicids ichnofabric (Fig. 12 A-C). Scolicids (*Scolicia*, *Bichordites*) bioturbating sands
576 (Facies Sm), silts and sandy muds (Facies Fm);

577 (2) *Palaeophycus* ichnofabric (Fig. 12 D-F). Numerous distinct burrows (e.g., *Planolites*,
578 *Palaeophycus*, *Schaubcylindrichnus* – morphotype A) bioturbating sands, silts and sandy muds (Facies
579 Sm, Fm);

580 (3) High bioturbation ichnofabric (Fig. 12 G-L). Homogeneous or mottled muds and silts
581 (Facies Fm). Distinct burrows are not always present.

582 Interpretation: High bioturbation intensity and homogeneous bioturbation are interpreted to reflect slow
583 sedimentation, stable, well oxygenated physico-chemical conditions (Taylor et al., 2003; Gingras et al.,
584 2011; Uchman and Wetzel, 2011). The ichnofabric classes of this group have been interpreted as
585 follows:

586 (1) Scolicids ichnofabric. The abundance in scolicids suggests oxic porewater with normal
587 marine salinities (de Gibert and Goldring, 2008; Buatois and Mángano, 2011), the possible influence of
588 bottom currents (Löwemark et al., 2006; Wetzel et al., 2011), restricted competition by organisms of
589 deeper burrowing tiers (Fu and Werner, 2000) and a good quantity and quality of food (Wetzel, 2010).
590 These environmental features are consistent with an upper shoreface to offshore depositional setting.

591 (2) *Palaeophycus* ichnofabric. This ichnofabric class presents similar features with respect to
592 the previously discussed ichnofabric class, but the higher bioturbation intensity and diversity suggest a
593 less stressed environment. This scenario suggests an offshore depositional environment influenced by
594 hyperpycnal flows.

595 (3) High bioturbation ichnofabric. With respect to the other ichnofabrics of the same group, this
596 ichnofabric presents the highest bioturbation intensity, probably indicating higher bioturbation rates,
597 lower sedimentation rates and a higher availability of food (see Wetzel and Uchman, 1998). These
598 features are interpreted to represent an oxic offshore environment.

599

600 **DISCUSSION**

601 **Palaeoenvironment of the Arda section**

602 In this section, the seven fining upward cycles (Fig. 2) have been interpreted in terms of
603 palaeoenvironments, integrating the results of sedimentology, body fossil palaeontology and ichnology
604 (Fig. 13).

605 *Cycle 0*

606 Cycle 0 does not constitute a full cycle, as it lacks the complete facies sequence characterising cycles
607 I-VII (see paragraph 'Facies Association'). The presence of brachiopods, corals and echinoids
608 (Biofacies 3; 45.65-46.05 m) as well as the prevalence of high-bioturbation ichnofabric in this cycle
609 would suggest an offshore transition environment characterised by low hydrodynamic energy and low
610 sedimentation rate. However, oscillations to high-energy foreshore to shoreface settings with high
611 sedimentation rate do also occur, as testified by the presence of rheophilous molluscs in Biofacies 1
612 (37.05-43.25 m). In addition, it is noteworthy the presence (45.20-46.60 m) of a characteristic body of
613 cemented biocalcarene with abundant burrows (*Thalassinoides* ichnofabric). Different physical
614 conditions can be assumed for its formation such as reduced fine-grained terrigenous input or strong

615 bottom reworking by currents. The upward reduction of winnowing events restores the initial low-
616 energy conditions characterised by deposition of finer-grained sediments. Here, body fossils show,
617 besides a diagenetic dissolution of aragonitic shells, a high degradation (Biofacies 2; 44.90 m, 47.35-49
618 m), suggesting a high-energy setting winnowed by currents. In this cycle oxygen isotope values of
619 bivalve shells (Crippa et al., 2016) point at temperate-cold conditions, related to a mid-shelf
620 environment (around 50 metres of depth).

621 *Cycle I*

622 Cycle I is interpreted to reflect environmental conditions similar to those of the previous cycle, i.e.
623 prevailing offshore transition conditions. Specifically, with the exception of a thin sandstone bed in the
624 basal part, most of Cycle I is represented by monotonous fine-grained to laminated siltstones (Facies L)
625 deposited by suspension settling from decelerating hyperpycnal flows. Body and trace fossils record a
626 change in the environment; the lower part of the cycle accounts for lower shoreface to offshore
627 transition settings [Biofacies 2 (56.35-58.35 m) and high-bioturbation ichnofabric], whereas the middle
628 part records a temporary shift to shallower and higher-energy foreshore to shoreface settings [Biofacies
629 4 (59-70.02 m) and presence of the *Macaronichnus* and scolichids ichnofabrics]. The topmost part
630 testified a return to a deeper water setting [Biofacies 8 (80.30-91.40 m) and high-bioturbation
631 ichnofabric]. Although only few palaeotemperature data are available from body fossils of this cycle,
632 these suggest a temperate-cold water environment. Such interpretation is coherent with the presence of
633 *Macaronichnus*, a typical temperate to cold water indicator (Quiroz et al., 2010), and *Scolicia*, which,
634 though not exclusive, is common in temperate waters (Goldring et al., 2004, 2007).

635 *Cycle II*

636 Cycle II mainly documents offshore transition environments recording a cooling event. The basal part
637 of the cycle documents a shoreface environment characterised by high to high-fluctuating energy and
638 high sedimentation rate. This cycle includes coarse-grained deposits related to shear/drag forces exerted

639 by the overpassing long-lived turbulent (hyperpycnal) flow over coarse-grained materials lying on the
640 flow bottom. High-density flows triggered by river floods can mix and deposit skeletal remains from
641 different shallow-water communities. The poor preservation of body fossils in Biofacies 10 (92.50-
642 98.30 m), the abrupt changes in ichnofabric, the presence of mud clasts and of reworked vegetal debris,
643 besides field observations, all indicate the presence in this interval (91.40-98 m) of a channel cutting
644 obliquely (direction south-southwest – north-northeast) the main succession and discharging fresh
645 water and sediments. Aside from this interval, sedimentology and trace fossils document offshore
646 transition environments, whereas body fossils record a shallowing upward trend, passing from an
647 offshore transition environment characterised by low-energy and low sedimentation rate (Biofacies 8;
648 101-104.10 m) to a shoreface setting with higher energy (Biofacies 4; 106.50-111.60 m). From a
649 palaeoclimatic point of view the first occurrence of the “northern guest” *Arctica islandica* (103.70 m)
650 and the abundant presence of *Macaronichnus* (94 m), mark the beginning of a climatic cooling in the
651 area, which is further supported by bivalve shell oxygen isotope composition (Crippa et al., 2016).

652 *Cycles III-VI*

653 Cycles III to VI show a more regular organization; each cycle records a deepening upward trend (from
654 foreshore-shoreface to offshore transition settings) and a likewise decrease in hydrodynamic energy
655 and sedimentation rate. Each cycle frequently has an erosive base and starts with conglomerates or rip-
656 up mud clasts (Facies B), followed above by sandstones either massive or stratified (Facies S). Here,
657 low bioturbation ichnofabric indicates brackish conditions, possibly caused by direct fluvial discharge
658 of fresh water and sediments by hyperpycnal flows. This is also supported by the presence of Biofacies
659 10 (170-194.10 m; 208.40-210.40 m) in Cycles V and VI; this biofacies contains an ecologically mixed
660 fauna and specimens showing a poor preservation, both evidence indicating a high-energy environment
661 affected by high density flows triggered by river floods which mix skeletal remains from different
662 environments. In Cycles III-VI transported body fossil assemblages and evidence of density flows

663 become more frequent; this means more river discharge and thus more terrigenous input into the
664 Palaeo-Adriatic basin. The increase in the tectonic uplift and erosion of the Apennines after 1.80 Ma
665 (e.g., Amorosi et al., 1996; Bartolini et al., 1996; Argnani et al., 1997, 2003; Dominici, 2001, 2004),
666 the proximity to the coast and possibly the climatic deterioration (e.g., increased precipitations and/or
667 increased ice melting during summer and more ice growth during winter) may account for the observed
668 increment of hyperpycnal flows in these cycles. The top of each cycle records fully marine conditions
669 with typical faunal associations/ichnofabrics of low-energy settings [Biofacies 7 (146.55-167.90 m,
670 196-207 m), high bioturbation ichnofabric)], reflecting the normal settling when the flow completely
671 stops or the sedimentation in a distal portion of the delta system.

672 Cycle V is particularly rich in scoliciid-dominated ichnofabrics. The sedimentological evidence for
673 hyperpycnal flows may indicate that *Scolicia*-dominated ichnofabrics are a proxy for extrabasinal
674 turbidites *sensu* Zavala and Arcuri (2016), such as those deposited by hyperpycnal flows. This
675 hypothesis is plausible as *Scolicia* is correlated with the abundance of food (Wetzel, 2010) and
676 extrabasinal turbidites are rich in phytodetritus because they originated from the continent (Zavala and
677 Arcuri, 2016). By contrast, intrabasinal turbidites originated within the marine basin and are therefore
678 less rich in phytodetritus (Zavala and Arcuri, 2016). Further case studies are required to test this
679 hypothesis.

680 Palaeoclimatic indicators mainly suggest temperate water, although in a few levels, oxygen isotopes
681 from bivalve shells and evidence from trace fossils (*Macaronichnus*) indicate lower water
682 temperatures, confirming the change towards cooler climates, affecting the Palaeo-Adriatic after the
683 arrival of the “northern guests”. In Cycle III, trace fossils record high-frequency climate fluctuations;
684 abundant *Ophiomorpha*, an ichnological indicator of warm climate, are present at little stratigraphic
685 distance from *Macaronichnus*-dominated horizons.

686 *Cycle VII*

687 Cycle VII represents the last marine cycle of the Arda succession before the establishment of a
688 continental environment with freshwater molluscs and vertebrate faunas (Bona and Sala, 2016; Monesi
689 et al., 2016); it documents a foreshore to upper shoreface environment characterised by high
690 hydrodynamic energy and high sedimentation rate, due to discharge by fluvial floods. This cycle is
691 characterised by the dominance of ichnofabrics related to brackish water (low bioturbation ichnofabric,
692 few sharp burrows-smooth burrows ichnofabrics). Increased freshwater input, and thus salinity dilution,
693 is also indicated by the presence of Biofacies 5 (230.80-237 m), recording from 230.80 m to the top the
694 only occurrence of *Glycymeris insubrica*, a species which tolerates salinity variations (e.g., Malatesta,
695 1974; Lozano Francisco et al., 1993; Raineri, 2007; Crnčević et al., 2013). At the top of the succession,
696 Crippa et al. (2016) observed the presence of abundant brackish-water benthic foraminifera and low
697 oxygen isotope ratios in bivalve shells, indicating salinity reduction due to freshwater river discharge.
698 All these evidence, together with the presence of frequent bed-load deposits (Facies B), indicate a
699 foreshore to upper shoreface environment for this part of the section.

700

701 **Regional significance of the Arda section**

702 The Arda sedimentary succession represents a valuable case study as it offers the rare opportunity to
703 study depositional dynamics through phases of strong natural climate change within a tectonically
704 active setting. The stratigraphic and palaeontological investigation presented for the Arda section
705 highlights the importance of integrated studies to disentangle the effects of climate and tectonic
706 processes acting in structuring sedimentary successions during the early Pleistocene. In this respect, the
707 overall regressive trend of the marine part of Arda section, consisting of offshore/prodelta (Cycles 0-II)
708 passing to prodelta/delta front (Cycles III-IV) and to intertidal/coastal (Cycle VII) stacked successions,
709 can be directly related to deformation phases of the local fronts of Apennine mountains; this is
710 represented by the change in the dip of the bedding from 20° in the stratigraphically lower part of the

711 section up to $<5^\circ$ in the upper part. While tectonic and climatic forcings are acting simultaneously,
712 regional studies (e.g., Gunderson et al., 2014) evidenced as the early Pleistocene (from about 1.60 till
713 1.10 Ma) structuring of this sector of the northern Apennines has been characterized by unsteady but
714 rapid and intense deformation. This specified interval of time encompasses the entire marine
715 sedimentation along the Arda section (see Geological Setting; Crippa et al., 2016). In addition, overall
716 regressive trends were already documented for few other successions outcropping along the north-
717 eastern margin of the Apennines, such as the Enza and Stirone River sections (e.g., Pelosio and Raffi,
718 1977; Dominici, 2001; Gunderson et al., 2014).

719 The cyclothemic nature of the sedimentary succession retains an expression of climatic changes that
720 occurred during the early Pleistocene and was modulated by the morphology of the basin (see
721 Dominici, 2001). Specifically, cyclic stacking pattern of fan-delta forestepping/backstepping episodes
722 described here were produced primarily by the onset and disappearance of local climatic conditions
723 favouring the development of catastrophic flooding through time (see other geologic examples in
724 Weltje and de Boer, 1993; Mutti et al., 1996). Our results correlate well with regional changes at higher
725 temporal frequencies, recording, besides the Apennine uplift, the same evolutionary history of coeval
726 successions in the Castell'Arquato basin and the Palaeo-Adriatic region (e.g., Stirone and Enza River
727 sections; Papani and Pelosio, 1962; Dominici, 2001, 2004; Gunderson et al., 2014). The analyses of the
728 biota and of their traces record not only local but also global climate changes. The occurrence of the
729 “northern guest” bivalve *A. islandica*, of *Macaronichnus* trace fossil, and of the “northern guests”
730 foraminifera *Hyalinea balthica* and *Neogloboquadrina pachyderma* left coiling (Crippa et al., 2016) in
731 the section, testified a climatic deterioration, i.e. cooling, which represents an expression of the climatic
732 changes occurring during the early Pleistocene, leading to the onset and establishment of Middle and
733 Upper Pleistocene continental glaciations.

734

735 **The multidisciplinary method: advantages and disadvantages**

736 The methodological significance of this study is to provide a multidisciplinary approach to
737 palaeoenvironmental reconstructions. The ecosystem evolution is affected by many different factors;
738 instead of just looking at one factor, we followed an integrated approach for the understanding of past
739 environments, integrating three different tools (sedimentology, body and trace fossil palaeontology).
740 The practical application of a multidisciplinary approach in palaeoenvironmental reconstructions
741 revealed some methodological advantages and disadvantages. One of the main advantages in applying
742 this method is the possibility to investigate, from different point of views, the ecosystems in detail,
743 obtaining a more complete and reliable picture of past environments. The use of a single tool, besides
744 giving a one side perspective, may be affected by biases specific to the tool itself, which can be avoided
745 or compensated for when using two or more tools. However, in employing different tools, data may
746 also disagree. Disagreements are generally due to different sampling strategies or to problems intrinsic
747 to the tools themselves, for example the lack of continuity in the recorded data along the succession and
748 thus a lower resolution scale of analysis, which does not allow to identify small variations. In the case
749 of the Arda River section, data from sedimentology and body fossils have shown a lower resolution in
750 the scale of analysis compared to trace fossils. For practical reasons, sedimentology, body fossil
751 palaeontology and ichnology involve different sampling schemes, characterised by different
752 resolutions, which also affect the results of the analysis. In some cases, this has led to possible
753 misinterpretations and disagreements between the different tools used; on the other hand, the higher
754 resolution shown by trace fossils has allowed to identify changes at a finer scale of analysis,
755 highlighting also the smallest environmental variation. Generally, we noted that these three different
756 approaches complement one another quite well and compensate for their respective defects, giving
757 strength and robustness to the obtained results, besides a more complete and exhaustive picture of past
758 ecosystems.

759 The geological record provides a number of different settings and locations within different time
760 intervals, where this multidisciplinary approach can be applied. Elements required are well exposed,
761 continuous and age constrained sedimentary successions rich of fossils (micro-, macro- and/or trace
762 fossils) and two, although three or more are preferred, different tools on which to base the
763 palaeoenvironmental reconstruction. The use of a multidisciplinary approach would greatly improve
764 the resolution of past environment reconstructions and should be applied more frequently for these
765 purposes, taking advantages of the numerous opportunities that the geological record provides.

766

767 **CONCLUSION**

768 The detailed multidisciplinary study presented here (sedimentology, body and trace fossils) has proved
769 to be a powerful tool for resolving palaeoenvironmental dynamics recorded in sedimentary succession
770 from collisional margins during time intervals of climate change. The palaeoenvironmental evolution
771 of the marine Arda River section has been interpreted taking into account the interplay between
772 tectonics and climatic factors. Based upon sedimentology, body fossils and trace fossils, it corresponds
773 to a subaqueous extension of a fluvial system, originated in a tectonically active setting during phases
774 of advance of fan deltas affected by high-density flows triggered by river floods, which are an
775 expression of early Pleistocene climate changes. It documents a fully marine and well oxygenated
776 environment, bounded at the top by continental conglomerates indicating a major sea level drop and the
777 establishment of a continental environment; indeed, a general regressive trend is observed through the
778 section, passing from a prodelta (Cycles 0-II) to a delta front (Cycles III-IV) to an intertidal zone
779 (Cycle VII) settings. Lower order transgressive and regressive cycles with shifts from lower foreshore-
780 shoreface to offshore transition environments have been identified, with supposed water depths ranging
781 between 5 and 50 m. The hydrodynamic energy and the sedimentation rate are not constant through the
782 section, but they are influenced by hyperpycnal flows which caused an increase in terrigenous input

783 linked to fluvial floods, whose sediments are mainly supplied by an increase in the Apennine uplift and
784 erosion, especially after 1.80 Ma (e.g., Amorosi et al., 1996; Bartolini et al., 1996; Argnani et al., 1997,
785 2003; Dominici, 2001, 2004). The regressive trend and the climatic deterioration, i.e. cooling, recorded
786 through the section are an expression of the climatic changes occurring during the early Pleistocene;
787 our results correspond well with other studies of both global and local climatic/tectonic changes,
788 recording the same evolutionary history of coeval successions in the Castell'Arquato basin and the
789 Palaeo-Adriatic region.

790 The lower Pleistocene Arda River marine succession represents only one of the numerous case studies
791 provided by the geological record where to apply a multidisciplinary approach to interpret past
792 complex ecosystems in the frame of climate change and tectonic activity. A multi-approach analysis
793 based on the integration of sedimentological data, body and trace fossils would greatly improve the
794 resolution of palaeoenvironmental reconstructions and should be extended also to other geological
795 sites.

796

797 **ACKNOWLEDGEMENTS**

798 G. Crippa was supported by 2011 Italian Ministry PRIN Project to E. Erba. A. Baucon was supported
799 by the ROSAE project (www.rosaeproject.org). We warmly thank the Editors, S. Schneider and an
800 anonymous reviewer for their constructive comments that improved the paper. L. Angiolini and M.
801 Marini are thanked for constructive discussions. M. Marini is also warmly thanked for English check.

802

803 **REFERENCES**

804 Amorosi, A., Farina, M., Severi, P., Preti, D., Caporale, L., Di Dio, G., 1996. Genetically related
805 alluvial deposits across active fault zones: an example of alluvial fan-terrace correlation from the upper
806 Quaternary of the Southern Po Basin Italy. *Sedimentary Geology* 102, 275–295.

807

808 Argnani, A., Bernini, M., Di Dio, G.M., Papani, G., Rogledi, S., 1997. Stratigraphic record of crustal-
809 scale tectonics in the Quaternary of the Northern Apennines (Italy). *Il Quaternario* 10, 595–602.

810

811 Argnani, A., Barbacini, G., Bernini, M., Camurri, F., Ghielmi, M., Papani, G., Rizzini, F., Rogledi, S.,
812 Torelli, L., 2003. Gravity tectonics driven by Quaternary uplift in the Northern Apennines: insights
813 from the La Spezia-Reggio Emilia geo-transect. *Quaternary International* 101–102, 13–26.

814

815 Artoni, A., Bernini, M., Papani, G., Rizzini, F., Barbacini, G., Rossi, M., Rogledi, S., Ghielmi, M.,
816 2010. Mass-transport deposits in confined wedge-top basins: surficial processes shaping the messinian
817 orogenic wedge of Northern Apennine of Italy. *Italian journal of geosciences* 129(1), 101-118.

818

819 Bartolini, C., Caputo, R., Pieri, M., 1996. Pliocene–Quaternary sedimentation in the Northern
820 Apennine Foredeep and related denudation. *Geological Magazine* 133, 255–273.

821

822 Bates, C., 1953. Rational theory of delta formation. *AAPG Bulletin* 37, 2119–2162.

823

824 Baucon, A., Bordy, E., Brustur, T., Buatois, L.A., De, C., Duffin, C., Felletti, F., Lockley, M., Lowe,
825 P., Mayor, A., Mayoral, E., Muttoni, G., Carvalho, C.N. De, Santos, A., Seike, K., Song, H., Turner, S.,
826 2012. A History of Ideas in Ichnology, in: Knaust, D., Bromley, R.G. (Eds.), *Trace Fossils as Indicators*
827 *of Sedimentary Environments. Developments in Sedimentology* 64. Elsevier, Amsterdam, pp. 3–43.

828 doi:10.1016/B978-0-444-53813-0.00001-0.

829

830 Baucon, A., Ronchi, A., Felletti, F., Neto de Carvalho, C., 2014. Evolution of Crustaceans at the edge

831 of the end-Permian crisis: ichnonetwork analysis of the fluvial succession of Nurra (Permian-Triassic,
832 Sardinia, Italy). *Palaeogeography Palaeoclimatology Palaeoecology* 410, 74–103.

833

834 Bertini, A., 2010. Pliocene to Pleistocene palynoflora and vegetation in Italy: state of the art.
835 *Quaternary International* 225 (1), 5–24.

836

837 Bhattacharya, J.P., MacEachern, J.A., 2009. Hyperpycnal Rivers and Prodeltaic Shelves in the
838 Cretaceous Seaway of North America. *Journal of Sedimentary Research* 79, 184–209.
839 doi:10.2110/jsr.2009.026.

840

841 Bona, F., Sala, B., 2016. Villafranchian-Galerian mammal faunas transition in South- Western Europe.
842 The case of the late early Pleistocene mammal fauna of the Frantoio locality, Arda River
843 (Castell'Arquato, Piacenza, Northern Italy). *Geobios* 49 (5), 329-347.

844

845 Bottjer, D.J., Droser, M.L., 1991. Ichnofabric and Basin Analysis. *Palaios* 6, 199–205.

846

847 Brenchley, P. J., Harper, D., 1998. *Palaeoecology: Ecosystems, environments and evolution*, Chapman
848 and Hall, London.

849

850 Brett, C.E., Baird, G.C., 1986. Comparative taphonomy: a key to paleoenvironmental interpretation
851 based on fossil preservation. *Palaios* 1, 207-227.

852

853 Bromley, R.G., 1996. *Trace fossils: biology, taphonomy and applications*, Second. ed. Chapman &
854 Hall, London.

855

856 Browne G.H., Naish T.R. 2003. Facies development and sequence architecture of a late Quaternary
857 fluvial-marine transition, Canterbury Plains and shelf, New Zealand: implications for forced regressive
858 deposits. *Sedimentary Geology* 158, 57-86.

859

860 Bruno, L., Amorosi, A., Severi, P., Costagli, B., 2017. Late Quaternary aggradation rates and
861 stratigraphic architecture of the southern Po Plain, Italy. *Basin Research* 29, 234-248.

862

863 Buatois, L.A., Gingras, M.K., MacEachern, J., Magano, G.M., Zonneveld, H.-P., Pemberton, S.G.,
864 Netto, R.G., Martin, A.J., 2005. Colonization of Brackish-Water Systems through Time: Evidence from
865 the Trace-Fossil Record. *Palaios* 20, 321–347. doi:10.2110/palo.2004.p04-32

866

867 Buatois, L.A., Mángano, M.G., 2011. *Ichnology: Organism-Substrate Interactions in Space and Time*.
868 Cambridge University Press, Cambridge New York.

869

870 Calabrese, L., Di Dio, G., 2009. Note Illustrative della Carta Geologica d'Italia alla scala 1: 50.000,
871 foglio 180 “Salsomaggiore Terme”. Servizio Geologico d'Italia-Regione Emilia Romagna, Roma.

872

873 Carminati, E., Doglioni, C., 2012. Alps vs. Apennines: the paradigm of a tectonically asymmetric
874 Earth. *Earth Science Reviews* 112, 67-96.

875

876 Carruba, S., Casnedi, R., Felletti, F., 2004. From seismic to bed: surface–subsurface correlations within
877 the turbiditic Cellino Formation (central Italy). *Petroleum Geoscience* 10(2), 131-140.

878

879 Cau, S., Taviani, M., Manzi, V., Roveri, M., 2013. Paleoecological, bio-sedimentological and
880 taphonomic analysis of Plio-Pleistocene biocalcarene deposits from northern Apennines and Sicily
881 (Italy). *Journal of Mediterranean Earth Sciences Special Issue*, 35-37
882

883 Cau, S., Roveri, M., Taviani, M., 2017. Anatomy of biocalcarene units in the Plio-Pleistocene record
884 of the Northern Apennines (Italy). *Geophysical Research Abstracts* 19, EGU2017-19478
885

886 Ceregato, A., Raffi, S., Scarponi, D., 2007. The circalittoral/bathyal in the Middle Pliocene of Northern
887 Italy: the case of the *Korobkovia oblonga*–*Jupiteria concava* paleocommunity type. *Geobios* 40, 555–
888 572.
889

890 Ciancherotti, A.D., Crispino, P., Esu, D., 1997. Paleocology of the non-marine molluscs of the
891 Pleistocene Stirone River sequence (Emilia, Northern Italy). *Bollettino della Società Paleontologica*
892 *Italiana* 36, 303-310.
893

894 Cigala Fulgosi, F., 1976. *Dicerorhinus hemitoechus* (Falconer) del post-Villafranchiano fluvio lacustre
895 del T. Stirone (Salsomaggiore, Parma). *Bollettino della Società Paleontologica Italiana* 15(1), 59–72.
896

897 Clifton, H.E., Thompson, J.K., 1978. *Macaronichnus segregatis*: a feeding structure of shallow marine
898 polychaetes. *Journal of Sedimentary Petrology* 48, 1293–1302. doi:10.1306/212F7667-2B24-11D7-
899 8648000102C1865D.
900

901 Coelho, V.R., Rodrigues, S. de A, 2001. Trophic behaviour and functional morphology of the feeding
902 appendages of the laomediid shrimp *Axianassa australis* (Crustacea: Decapoda: Thalassinidea). *Journal*

903 of the Marine Biological Association of the United Kingdom 81: 441-454.

904

905 Combourieu-Nebout, N., Bertini, A., Russo-Ermolli, E., Peyron, O., Klotz, S., Montade, V., Fauquette,

906 S., Allen, J., Fusco, F., Goring, S., Huntley, B., Joannin, S., Lebreton, V., Magri, D., Martinetto, E.,

907 Orain, R., Sadori, L., 2015. Climate changes in the central Mediterranean and Italian vegetation

908 dynamics since the Pliocene. *Review of Palaeobotany and Palynology* 218, 127–147.

909

910 Crippa, G., Raineri, G., 2015. The genera *Glycymeris*, *Aequipecten* and *Arctica*, and associated mollusk

911 fauna of the Lower Pleistocene Arda River section (Northern Italy). *Rivista Italiana di Paleontologia e*

912 *Stratigrafia* 121 (1), 61–101.

913

914 Crippa G., Angiolini L., Bottini C., Erba E., Felletti F., Frigerio C., Hennissen J.A.I., Leng M.J.,

915 Petruzzo M.R., Raffi I., Raineri G., Stephenson M.H., 2016. Seasonality fluctuations recorded in fossil

916 bivalves during the early Pleistocene: Implications for climate change. *Palaeogeography*

917 *Palaeoclimatology Palaeoecology* 446, 234–251.

918

919 Crnčević, M., Balić, D.E., Pećarević, M., 2013. Reproductive cycle of *Glycymeris nummaria*

920 (Linnaeus, 1758) (Mollusca: Bivalvia) from Mali Ston Bay, Adriatic Sea, Croatia. *Scientia Marina* 77

921 (2), 293–300.

922

923 de Gibert, J., Goldring, R., 2008. Spatangoid-produced ichnofabrics (Bateig Limestone, Miocene,

924 Spain) and the preservation of spatangoid trace fossils. *Palaeogeography Palaeoclimatology*

925 *Palaeoecology* 270, 299–310. doi:10.1016/j.palaeo.2008.01.031

926

927 Dodd, J.R., Stanton, R.J., 1990. *Paleoecology: concepts and applications*. John Wiley & Sons.
928

929 Dominici, S., 2001. Taphonomy and paleoecology of shallow marine macrofossil assemblages in a
930 collisional setting (late Pliocene–early Pleistocene, western Emilia, Italy). *Palaios* 16, 336–353.
931

932 Dominici, S., 2004. Quantitative Taphonomy in Sandstones from an Ancient Fan Delta System (Lower
933 Pleistocene, Western Emilia, Italy). *Palaios* 19, 193–205.
934

935 Felletti, F., Carruba, S., Casnedi, R., 2009. Sustained turbidity currents: evidence from the Pliocene
936 Periadriatic foredeep (Cellino Basin, Central Italy). *External Controls on Deep-Water Depositional*
937 *Systems*. SEPM, Special Publication 92, 325-346.
938

939 Frey, R.W., Howard, J.D., Pryor, W.A., 1978. *Ophiomorpha*: its morphologic, taxonomic, and
940 environmental significance. *Palaeogeography Palaeoclimatology Palaeoecology* 23, 199–229.
941

942 Fu, S., Werner, F., 2000. Distribution, ecology and taphonomy of the organism trace, *Scolicia*, in
943 northeast Atlantic deep-sea sediments. *Palaeogeography Palaeoclimatology Palaeoecology* 156, 289–
944 300.
945

946 Fürsich, F.T., 1978. The influence of faunal condensation and mixing on the preservation of fossil
947 benthic communities. *Lethaia* 11, 243–250.
948

949 Fusco, F., 2010. *Picea + Tsuga* pollen record as a mirror of oxygen isotope signal? An insight into the
950 Italian long pollen series from Pliocene to Early Pleistocene. *Quaternary International* 225 (1), 58–74.

951

952 Ghibaudo, G., 1992. Subaqueous sediment gravity flow deposits: practical criteria for their field
953 description and classification. *Sedimentology* 39(3), 423-454.

954

955 Gingras, M.K., MacEachern, J. A., Dashtgard, S.E., 2011. Process ichnology and the elucidation of
956 physico-chemical stress. *Sedimentary Geology* 237, 115–134. doi:10.1016/j.sedgeo.2011.02.006

957

958 Goldring, R., Cadée, G., D'Alessandro, A., de Gibert, J.M., Jenkins, R., Pollard, J.E., 2004. Climatic
959 control of trace fossil distribution in the marine realm, in: McIlroy, D. (Eds.), *The Application of*
960 *Ichnology to Palaeoenvironmental and Stratigraphic Analysis*. Geological Society of London, Special
961 Publications 228, London, pp. 77–92.

962

963 Goldring, R., Cadée, G., Pollard, J.E., 2007. Climatic Control of Marine Trace Fossil Distribution, in:
964 Miller III, W. (Eds.), *Trace Fossils. Concepts, Problems, Prospects*. Elsevier B.V., Amsterdam, pp.
965 159–171.

966

967 Gregory, M.R., Campbell, K.A., Zuraida, R., Martin, A.J., 2006. Plant Traces Resembling *Skolithos*.
968 *Ichnos* 13 (4), 205-216.

969

970 Gunderson, K.L., Pazzaglia, F.J., Picotti, V., Anastasio, D.A., Kodama, K.P., Rittenour, T., Frankel,
971 K.F., Ponza, A., Berti, C., Negri, A., Sabbatini, A., 2014. Unraveling tectonic and climatic controls on
972 synorogenic growth strata (Northern Apennines, Italy). *Geological Society of America Bulletin* 126(3-
973 4), 532-552.

974

975 Hauck, T.E., Dashtgard, S.E., Pemberton, S.G., Gingras, M.K., 2009. Brackish-water ichnological
976 trends in a micro- tidal barrier island/embayment system, Kouchibouguac National Park, New
977 Brunswick, Canada. *Palaios* 24, 478– 496. doi:10.2110/palo.2008.p08-056r
978

979 Knaust, D., 2017. *Atlas of Trace Fossils in Well Core*. Springer, Cham, 209 pp.
980

981 Kowalewski, M., Wittmer, J.M., Dexter, T.A., Amorosi, A., Scarponi, D., 2015. Differential response
982 of marine communities to natural and anthropogenic changes. *Proceedings of the Royal Society of*
983 *London B* 282, doi:10.1098/rspb.2014.2990
984

985 Książkiewicz, M., 1954. Uwarstwienie frakcjonalne i laminowane we fliszu karpackim [Graded and
986 laminated bedding in the Carpathian Flysch]. *Rocznik Polskiego Towarzystwa Geologicznego* 22, 399–
987 471. (In Polish, English summary).
988

989 Leaman, M., Mcilroy, D., Herringshaw, L.G., Boyd, C., Callow, R.H.T., 2015. What does
990 *Ophiomorpha irregulaire* really look like? *Palaeogeography Palaeoclimatology Palaeoecology* 439,
991 38–49. doi:10.1016/j.palaeo.2015.01.022
992

993 Lobza, V., Schieber, J., 1999. Biogenic sedimentary structures produced by worms in soupy, soft muds:
994 observations from the Chattanooga Shale (Upper Devonian) and experiments. *Journal of Sedimentary*
995 *Research* 69, 1041–1049.
996

997 Löwemark, L., Lin, Y., Chen, H.-F., Yang, T.-N., Beier, C., Werner, F., Lee, C.-Y., Song, S.-R., Kao,
998 S.-J., 2006. Sapropel burn-down and ichnological response to late Quaternary sapropel formation in

999 two ~400 ky records from the eastern Mediterranean Sea. *Palaeogeography Palaeoclimatology*
1000 *Palaeoecology* 239, 406–425. doi:10.1016/j.palaeo.2006.02.013.

1001

1002 Lozano Francisco, M.C., Vera Pelaez, J.L., Guerra Merchan, A., 1993. *Arcoïda (Mollusca, bivalvia)*
1003 *del Plioceno de la provincia de Málaga, España. Treballs del Museu de Geologia de Barcelona* 3, 157–
1004 188.

1005

1006 MacEachern, J.A., Pemberton, S.G., Gingras, M.K., Bann, K.L., 2007, *The ichnofacies concept: a*
1007 *fifty-year retrospective*, in: Miller III, W. (eds), *Trace Fossils. Concepts, Problems, Prospects*,
1008 Elsevier, pp. 50-75.

1009

1010 MacEachern, J.A., Bann, K.L., Gingras, M.K., Zonneveld, J.-P., Dashtgard, S., Pemberton, S.G., 2012.
1011 *The Ichnofacies Paradigm*. In: Knaust, D., Bromley, R.G. (Eds.) *Trace Fossils as Indicators of*
1012 *Sedimentary Environments. Developments in Sedimentology* 64: 563-603

1013

1014 Malatesta, A., 1974. *Malacofauna pliocenica umbra. Memoria per servire alla descrizione della Carta*
1015 *Geologica d'Italia* 13, 1–490.

1016

1017 Mancini, M., Moscatelli, M., Stigliano, F., Cavinato, G. P., Marini, M., Pagliaroli, A., Simionato, M.,
1018 2013. *Fluvial facies and stratigraphic architecture of Middle Pleistocene incised valleys from the*
1019 *subsoil of Rome (Italy). Journal of Mediterranean Earth Sciences (Special Issue)*, 89-93.

1020

1021 Marini, M., Milli, S., Rossi, M., De Tomasi, V., Meda, M., & Lisi, N., 2013. *Multi-scale*
1022 *characterization of the Pleistocene-Holocene Tiber delta deposits as a depositional analogue for*

1023 hydrocarbon reservoirs. *Journal of Mediterranean Earth Sciences (Special Issue)*, 103, 109.

1024 Martinelli, J.C., Soto, L.P., González, J., Rivadeneira, M.M., 2017. Benthic communities under
1025 anthropogenic pressure show resilience across the quaternary. *Royal Society Open Science*, 4 (9),
1026 170796.

1027

1028 Martínez-García, B., Rodríguez-Lázaro, J., Pascual, A., Mendicoa, J., 2015. The “northern guests” and
1029 other palaeoclimatic ostracod proxies in the late quaternary of the Basque basin (S bay of Biscay).
1030 *Palaeogeography Palaeoclimatology Palaeoecology* 419, 100–114.

1031

1032 Massari, F., Chiocci, F., 2006. Biocalcarene and mixed cool-water prograding bodies of the
1033 Mediterranean Pliocene and Pleistocene: architecture, depositional setting and forcing factors.
1034 *Geological Society, London, Special Publications* 255.1, 95-120.

1035

1036 McIlroy, D., 2004. The application of ichnology to palaeoenvironmental and stratigraphic analysis.
1037 *Geological Society* 228, London, Special publications.

1038

1039 McIlroy, D., 2008. Ichnological analysis: The common ground between ichnofacies workers and
1040 ichnofabric analysts. *Palaeogeography Palaeoclimatology Palaeoecology* 270, 332–338.
1041 doi:10.1016/j.palaeo.2008.07.016

1042

1043 Milli, S., Mancini, M., Moscatelli, M., Stigliano, F., Marini, M., Cavinato, G. P., 2016. From river to
1044 shelf, anatomy of a high-frequency depositional sequence: The Late Pleistocene to Holocene Tiber
1045 depositional sequence. *Sedimentology* 63(7), 1886-1928.

1046

1047 Monegatti, P., Raffi, S., Roveri, M., Taviani, M., 2001. One day trip in the outcrops of Castell'Arquato
1048 Plio–Pleistocene Basin: from the Badlands of Monte Giogo to the Stirone River. *Paleobiogeography
1049 and Paleoecology 2001 International Conference, Excursion Guidebook, Università di Parma, Parma,*
1050 *pp. 26.*

1051

1052 Monesi, E., Muttoni, G., Scardia, G., Felletti, F., Bona, F., Sala, B., Tremolada, F., Francou, C.,
1053 Raineri, G., 2016. Insights on the opening of the Galerian mammal migration pathway from
1054 magnetostratigraphy of the Pleistocene marine–continental transition in the Arda River section
1055 (northern Italy). *Quaternary Research* 86 (2), 220–231.

1056

1057 Mulder, T., Syvitski, J.P.M., Migeon, S., Faugères, J.C., Savoye, B., 2003. Marine hyperpycnal flows:
1058 Initiation, behavior and related deposits. A review. *Marine and Petroleum Geology* 20, 861–882.

1059

1060 Mutti, E., Davoli, G., Tinterri, R., Zavala, C., 1996, The importance of ancient fluvio-deltaic systems
1061 dominated by catastrophic flooding in tectonically active basins: *Memorie di Scienze Geologiche*, 84,
1062 233–291.

1063

1064 Mutti, E., Tinterri, R., Di Biase, D., Fava, L., Mavilla, N., Angella, S., Calabrese, L., 2000. Delta-front
1065 facies associations of ancient flood-dominated fluvio-deltaic systems. *Revista Società Geologica de
1066 España* 13, 165–190.

1067

1068 Mutti, E., Tinterri, R., Benevelli, G., Di Biase, D., Cavanna, G., 2003. Deltaic, mixed and turbidite
1069 sedimentation of ancient foreland basins. *Marine and Petroleum Geology* 20, 733–755.

1070

1071 Nichols, G., 2009. Sedimentology and Stratigraphy. Second Edition. Wiley-Balckwell, Chichester.
1072

1073 Ori, G.G., Roveri, M., Vannoni, F., 1986. Plio-Pleistocene sedimentation in the Apenninic-Adriatic
1074 foredeep (Central Adriatic Sea, Italy). International Association of Sedimentologists, Special
1075 Publication 8, 183–198.
1076

1077 Papani, G., Pelosio, G. 1962 (1963). La serie plio-pleistocenica del Torrente Stirone (Parmense
1078 Occidentale). Bollettino della Società Geologica Italiana 81 (3), 293-325.
1079

1080 Pearson, N.J., Gabriela Mángano, M., Buatois, L.A., Casadío, S., Raising, M.R., 2013. Environmental
1081 variability of *Macaronichnus ichnofabrics* in Eocene tidal-embayment deposits of southern Patagonia,
1082 Argentina. Lethaia 46, 341–354. doi:10.1111/let.12012
1083

1084 Pelosio, G., Raffi, S., 1977. Preliminary remarks on mollusc assemblages of the Stirone river
1085 Pleistocene series (Parma Province, Northern Italy). X INQUA Congress, Birmingham, 1–19.
1086

1087 Pemberton, S.G., Spila, M., Pulham, A.J., Saunders, T., MacEachern, J.A., Robbins, D., Sinclair, I.K.,
1088 2001. Ichnology & Sedimentology of Shallow to Marginal Marine Systems. Geological Association of
1089 Canada, Short Course Notes Volume 15. AGMV Marquis, St. John's.
1090

1091 Pérès J.M., Picard J., 1964. Nouveau manuel de bionomie benthique de la Méditerranée. Recueil des
1092 Travaux de la Station Marine d'Endoume 31, 1-137.
1093

1094 Pieri, M., 1983. Three seismic profiles through the Po Plain, in: Bally, A.W. (Eds.), Seismic expression

1095 of structural styles: American Association of Petroleum Geologists, Studies in Geology Series 15,
1096 3.4.1/8–3.4.1/26.

1097

1098 Quiroz, L.I., Buatois, L.A., Mangano, M.G., Jaramillo, C. A., Santiago, N., 2010. Is the trace fossil
1099 *Macaronichnus* an indicator of temperate to cold waters? Exploring the paradox of its occurrence in
1100 tropical coasts. *Geology* 38, 651–654. doi:10.1130/G30140.1

1101

1102 Raffi, S., 1986. The significance of marine boreal molluscs in the Early Pleistocene faunas of the
1103 Mediterranean area. *Palaeogeography Palaeoclimatology Palaeoecology* 52, 267–289.

1104

1105 Raineri, G., 2007. *Riserva Naturale Geologica del Piacenziano: Appunti per un'Escursione, Parchi e*
1106 *Riserve dell'Emilia-Romagna* (52 p.).

1107

1108 Ricci Lucchi, F., 1986, Oligocene to Recent foreland basins of northern Apennines, in: Allen, P.H., and
1109 Homewood, P. (Eds.), *Foreland Basins: International Association of Sedimentologists, Special*
1110 *Publication No. 8*, 105–139.

1111

1112 Roveri, M., Taviani, M., 2003. Calcarenite and sapropel deposition in the Mediterranean Pliocene:
1113 shallow-and deep-water record of astronomically driven climatic events. *Terra Nova* 15(4), 279-286.

1114

1115 Roveri, M., Visentin, C., Argnani, A., Knezaurek, G., Lottaroli, F., Rossi, M., Taviani, M., Trincardi,
1116 F., Vigliotti, L., 1998. The Castell'Arquato Basin: high-resolution sequence stratigraphy and stratal
1117 patterns of an uplifting margin in the Apennines foothills (Italy), In: *SEPM–IAS Research Conference:*
1118 *Strata and Sequences on Shelves and Slopes* (M. Field, S. Berné, A. Colella, C. Nittrouer and F.

1119 Trincardi, eds), Sicily, September 15–19, 1998, Abstract Volume.

1120

1121 Savrda, C., Uddin, A., 2005. Large *Macaronichnus* and Their Behavioral Implications (Cretaceous
1122 Eutaw Formation, Alabama, USA). *Ichnos* 12, 1–9. doi:10.1080/10420940590914453.

1123

1124 Scarponi, D., Huntley, J. W., Capraro, L., Raffi, S., 2014. Stratigraphic paleoecology of the Valle di
1125 Manche section (Crotone Basin, Italy): a candidate GSSP of the Middle Pleistocene. *Palaeogeography
1126 Palaeoclimatology Palaeoecology* 402, 30-43.

1127

1128 Scarponi, D., Kusnerik, K., Azzarone, M., Amorosi, A., Bohacs, K., Drexler, T.M., Kowalewski, M.,
1129 2017a. Systematic vertical and lateral changes in quality and time resolution of the macrofossil record:
1130 insights from Holocene transgressive deposits, Po coastal plain, Italy. *Marine and Petroleum Geology*.
1131 doi:10.1016/j.marpetgeo.2017.03.031.

1132

1133 Scarponi, D., Azzarone, M., Kowalewski, M., Huntley, J.W., 2017b. Surges in trematode prevalence
1134 linked to centennial-scale flooding events in the Adriatic. *Scientific Reports*, 7 5732
1135 doi:10.1038/s41598-017-05979-6

1136

1137 Schäfer, W., 1956. Wirkungen der Benthos Organismen auf den jungen Schichtverband.
1138 *Senckenbergiana Lethaea* 37, 183–263

1139

1140 Schlirf, M., Uchman, A., 2005. Revision of the Ichnogenus *Sabellarifex* Richter, 1921 and its
1141 relationship to *Skolithos* Haldeman, 1840 and *Polykladichnus* Fürsich, 1981. *Journal of Systematic
1142 Palaeontology* 3, 115–131.

1143

1144 Seike, K., Yanagishima, S.I., Nara, M., Sasaki, T., 2011. Large *Macaronichnus* in modern shoreface
1145 sediments: Identification of the producer, the mode of formation, and paleoenvironmental implications.
1146 *Palaeogeography Palaeoclimatology Palaeoecology* 311, 224–229. doi:10.1016/j.palaeo.2011.08.023.

1147

1148 Seilacher, A., 1962. Paleontological studies on turbidite sedimentation and erosion. *The Journal of*
1149 *Geology* 70, 227–234.

1150

1151 Suess, E., 1883–1888, *Das Antlitz der Erde*: Tempsky and Freytag (eds.), (Prague (Czech Republic),
1152 Vienna (Austria) and Leipzig (Germany)).

1153

1154 Taviani, M., Roveri, M., Impiccini, R., Vigliotti, L., 1997. Segnalazione di Quaternario marino nella
1155 Val Chero (Appennino Piacentino). *Bollettino della Società Paleontologica Italiana*, 36, 331-338.

1156

1157 Taylor, P.D., Wilson, M.A., 2003. Palaeoecology and evolution of marine hard substrate communities.
1158 *Earth-Science Reviews* 62(1), 1-103.

1159

1160 Taylor, A., Goldring, R., Gowland, S., 2003. Analysis and application of ichnofabrics. *Earth-Science*
1161 *Reviews* 60, 227–259.

1162

1163 Tedesco, L.P., Wanless, H.R., 1991. Generation of Sedimentary Fabrics and Facies by Repetitive
1164 Excavation and Storm Infilling of Burrow Networks, Holocene of South Florida and Caicos Platform,
1165 B.W.I. *Palaios* 326-343.

1166

1167 Tinterri, R., 2007. The Lower Eocene Roda Sandstone (South-Central Pyrenees): an Example of a
1168 Flood-Dominated River-Delta System in a Tectonically Controlled Basin. *Rivista Italiana di*
1169 *Paleontologia e Stratigrafia* 113 (2), 223-255.
1170

1171 Tyson, R., Pearson, T.H., 1991. Modern and ancient continental shelf anoxia: An overview. *Geological*
1172 *Society, London, Special Publications* 58(1), 1-24
1173

1174 Uchman, A., Wetzel, A., 2011. Deep-Sea Ichnology: The Relationships Between Depositional
1175 Environment and Endobenthic Organisms, in: Huneke, H., Mulder, T. (Eds.), *Deep-Sea Sediments,*
1176 *Developments in Sedimentology* 63. Elsevier, Amsterdam, pp. 517–556. doi:10.1016/B978-0-444-
1177 53000-4.00008-1.
1178

1179 von Leesen, G., Beierlein, L., Scarponi, D., Schöne, B.R., Brey T., 2017. A low seasonality scenario in
1180 the Mediterranean Sea during the Calabrian (Early Pleistocene) inferred from fossil *Arctica islandica*
1181 shells. *Palaeogeography, Palaeoclimatology, Palaeoecology* 485, 706-714.
1182

1183 Weltje, G., de Boer, P.L., 1993. Astronomically induced paleoclimatic oscillations reflected in Pliocene
1184 turbidite deposits on Corfu (Greece): implications for the interpretation of higher order cyclicity in
1185 ancient turbidite systems. *Geology* 21(4), 307-310.
1186

1187 Wetzel, A., 2010. Deep-sea ichnology: Observations in modern sediments to interpret fossil
1188 counterparts. *Acta Geologica Polonica* 60, 125–138.
1189

1190 Wetzel, A., Uchman, A., 1998. Deep-Sea Benthic Food Content Recorded by Ichnofabrics: A

1191 Conceptual Model Based on Observations from Paleogene Flysch, Carpathians, Poland. *Palaios* 13,
1192 533-546.
1193

1194 Wetzel, A., Tjallingii, R., Wiesner, M.G., 2011. Bioturbational structures record environmental
1195 changes in the upwelling area off Vietnam (South China Sea) for the last 150,000years.
1196 *Palaeogeography Palaeoclimatology Palaeoecology* 311, 256–267. doi:10.1016/j.palaeo.2011.09.003.
1197

1198 Wittmer, J.M., Dexter, T.A., Scarponi, D., Amorosi, A., Kowalewski, M., 2014. Quantitative
1199 bathymetric models for late Quaternary transgressive-regressive cycles of the Po Plain, Italy. *The*
1200 *Journal of Geology* 122 (6), 649-670.
1201

1202 Williams, A., Brunton, C.H.C., Carlson, S.J., and 44 authors, 2000. Linguliformea, Craniiformea and
1203 Rhynconelliformea (part), in: Kaesler, R.L. (Eds.), *Treatise on Invertebrate Paleontology, Part H,*
1204 *Brachiopoda revised.* The Geological Society of America and The University of Kansas, Boulder,
1205 Colorado and Lawrence, Kansas, 2, pp. 423; 3, pp. 424–919.
1206

1207 Williams, A., Brunton, C.H.C., Carlson, S.J., and 44 authors, 2006. Rhynconelliformea (part), in:
1208 Kaesler, R.L. (Eds.), *Treatise on Invertebrate Paleontology, Part H, Brachiopoda revised.* The
1209 Geological Society of America and The University of Kansas, Boulder, Colorado and Lawrence,
1210 Kansas, 5, pp. 1689–2320.
1211

1212 Wysocka, A., Radwański, A., Górka, M. Bąbel, M., Radwańska, U., Złotnik, M., 2016. The Middle
1213 Miocene of the Fore-Carpathian Basin (Poland, Ukraine and Moldova). *Acta Geologica Polonica* 66,
1214 351-401. doi: 10.1515/agp-2016-0017

1215

1216 Zavala, C., Ponce, J., Drittanti, D., Arcuri, M., Freije, H., Asensio, M., 2006. Ancient lacustrine
1217 hyperpycnites: A depositional model from a case study in the Rayoso Formation (Cretaceous) of west-
1218 central Argentina. *Journal of Sedimentary Research* 76, 41–59. doi:10 .2110/jsr.2006.12.

1219

1220 Zavala, C., Arcuri, M., Di Meglio, M., Gamero Diaz, H., Contreras, C., 2011. A genetic facies tract for
1221 the analysis of sustained hyperpycnal flow deposits, in: Slatt, R.M., Zavala, C. (Eds.), *Sediment*
1222 *transfer from shelf to deep water—Revisiting the delivery system: AAPG Studies in Geology* 61, pp.
1223 31–5.

1224

1225 Zavala, C., Arcuri, M., 2016. Intrabasinal and extrabasinal turbidites: Origin and distinctive
1226 characteristics. *Sedimentary Geology* 337, 36-54.

1227

1228 **FIGURE CAPTIONS**

1229

1230 **Figure 1.** A) Geological sketch map of northern Italy showing the study area (modified after Crippa et
1231 al., 2016); B) Enlarged geological map of the Castell'Arquato basin with indication of the measured
1232 Arda River section (modified after Monesi et al., 2016). C) Photograph of a part of the outcrop along
1233 the Arda River section (metric interval on the stratigraphic section, Fig. 2: 120-140 m).

1234

1235 **Figure 2.** Detailed stratigraphic log of the Arda River section. Facies codes are listed in Table 1.

1236

1237 **Figure 3.** A-F) Facies related to bed-load processes (Facies B). This category includes different coarse-
1238 grained deposits related to shear/drag forces exerted by the overpassing long-lived turbulent

1239 (hyperpycnal) flow over coarse-grained material lying on the flow bottom. See Table 1 for facies codes
1240 and relative description. Corresponding metric intervals on the stratigraphic section (Fig. 2): A) 179.10
1241 m; B) 114 m; C) 94.10 m; D) 28.20 m; E) 224.80 m; F) 131.90 m.

1242

1243 **Figure 4.** A-F) Facies related to the collapse of suspended load (Facies S). This category mostly
1244 includes fine-grained sediments transported as suspended load, forming thick and commonly complex
1245 intervals that can be massive or display traction plus fallout sedimentary structures. See Table 1 for
1246 facies codes and relative description. Corresponding metric intervals on the stratigraphic section (Fig.
1247 2): A) 177.20 m; B) 134 m; C) 193.80 m; D) 230.60 m; E) 184.60 m; F) 194.20 m.

1248

1249 **Figure 5.** A) Facies related to flow lofting (Facies L). It is characterised by thin couplets of massive to
1250 laminated siltstones and mudstones (Fm), transported by the hyperpycnal flow, which accumulated by
1251 normal settling when the flow completely stopped (107.40 m). B) Cemented levels, rich in carbonate
1252 (CCB; 130.20 m). See Table 1 for facies codes and relative description. C) Erosional bedset-bounding
1253 surfaces (114 m). D) Rapid accumulation results in the common occurrence of water-escape features
1254 such as load cast and flame structures (184.60 m). E, F) Biocalcarenitic body (46 m). It forms
1255 prograding wedges typically displaying intense bioturbation. Foresets and bottomsets are characterised
1256 by dense accumulations of reworked shells.

1257

1258 **Figure 6.** Fossiliferous beds of the Arda succession. A) Articulated specimens of *Glycymeris inflata*
1259 (42 m, Biofacies 1, Cycle 0); B) Section of an articulated specimen of *Pinna* sp. (54.20 m, Biofacies
1260 10, Cycle I); C) Articulated specimen of *Pelecypora brocchii* in life position (57.35 m, Biofacies 2,
1261 Cycle I); D) Echinoid specimen (58.35 m, Biofacies 2, Cycle I); E) Shell accumulation mainly

1262 containing specimens of *Spisula subtruncata* (68.53 m, Biofacies 4, Cycle I); F) Life assemblage of
1263 articulated specimens of *Glycymeris insubrica* (133.90 m, Biofacies 9, Cycle IV).

1264

1265 **Figure 7.** Fossiliferous beds of the Arda succession. A) Bed with several specimens of *Aequipecten*
1266 *opercularis* (134.35 m, Biofacies 9, Cycle IV); B) Articulated specimen of *Arctica islandica* in life
1267 position and lacking internal sediment filling (224.30 m, Biofacies 6, Cycle VII); C) Specimens of
1268 *Chamelea gallina* with empty valves in life position (234 m, Biofacies 5, Cycle VI); D) Accumulation
1269 bed with mainly disarticulated bivalves (234.40 m, Biofacies 5, Cycle VII); E) Articulated specimens
1270 of *Glycymeris insubrica* (235.70 m, Biofacies 5, Cycle VII); F) Accumulation bed with articulated
1271 specimens of *Glycymeris insubrica*, representing the most abundant species at the top of the section
1272 (236.80 m, Biofacies 5, Cycle VII).

1273

1274 **Figure 8.** Taphonomic conditions of the body fossils; a: external or abapertural view, b: internal or
1275 apertural view. 1a,b) *Glycymeris inflata*, left valve; note the encrustation made by bryozoans and
1276 serpulids (ACG29bis-3, Biofacies 1, Cycle 0); 2a,b) *Pitar rudis*, right valve; note the hole of a
1277 bioerosion reaching the internal part of the valve (ACG106, Biofacies 7, Cycle IV); 3a,b) *Aequipecten*
1278 *opercularis*, right valve; the valve is encrusted by serpulids only in the external part (ACG27bis-6,
1279 Biofacies 1, Cycle 0); 4a,b) *Naticarius stercusmuscarum*, the original color pattern is preserved
1280 (ACG29bis-20, Biofacies 1, Cycle 0); 5a,b) *Peronidia albicans*, right valve; the finer ornamentation
1281 and the color pattern are preserved (ACG53-4, Biofacies 4, Cycle I); 6a,b) *Flexopecten glaber*, left
1282 valve; the finer ornamentation is preserved (ACG80-4, Biofacies 4, Cycle II); 7a,b) *Acanthocardia*
1283 *tuberculata*, right valve; note the attempt of a bioeroding organism to perforate the shell (ACG94,
1284 Biofacies 9, Cycle IV); 8a,b) *Aequipecten opercularis*, right valve; the finer ornamentation is well
1285 preserved (ACG104-2, Biofacies 7, Cycle IV); 9a,b) *Dosinia lupinus*, right valve; note the original

1286 color pattern (ACG235, Biofacies 10, Cycle VI); 10a,b) *Aequipecten opercularis*, left valve; the shell is
1287 encrusted by bryozoans both in the internal and external part (ACG238, Biofacies 10, Cycle VI); 11a,b)
1288 *Glycymeris insubrica*, left valve; the original color pattern is preserved (ACG197-5, Biofacies 10,
1289 Cycle V); 12a,b) *Flexopecten glaber*, right valve; the bioerosion does not perforate the entire thickness
1290 of the shell (ACG250, Biofacies 5, Cycle VII); 13a,b) *Dosinia lupinus*, right valve; hole made by
1291 bioeroding organisms (ACG201, Biofacies 10, Cycle V); 14a,b) *Callista chione*, right valve; note the
1292 preservation of the glossy periostracum (ACG197, Biofacies 10, Cycle V).

1293

1294 **Figure 9.** Ichnofabric group 1. A) *Ophiomorpha* ichnofabric. B) Close-up of A showing a specimen of
1295 *Ophiomorpha*, parallel lamination and concave-up shells. C) *Ophiomorpha* with a robust constructional
1296 lining, indicating high-energy conditions. D) *Macaronichnus* ichnofabric. E) *Macaronichnus*
1297 ichnofabric cross-cut by “Lined light filled burrows” (*Ophiomorpha?*). F) Intensely bioturbated
1298 *Macaronichnus* ichnofabric with a significant contribution from other undetermined ichnotaxa.

1299

1300 **Figure 10.** Ichnofabric group 2. A) Few sharp burrows-smooth burrows ichnofabric. B) Homogeneous
1301 suite represented by biogenic structures with poorly defined wall bioturbating a mud layer. C) Sharp
1302 burrows suite represented by a sharp-walled trace that bioturbated a mud layer. D) Sharp burrows-
1303 smooth burrows ichnofabric. E) Close-up of E showing several “sharp-walled traces”. F)
1304 *Schaubcylindrichnus?* (morphotype A). G) Scolicid-sharp burrows ichnofabric. H) Close-up of G
1305 showing a scolicid and abundant vegetal debris.

1306

1307 **Figure 11.** Ichnofabric group 3. A) *Lockeia* ichnofabric represented by numerous specimens of
1308 *Lockeia*; bedding plane view. B) *Ophiomorpha* preserved in cemented layers. C) *Thalassinoides*

1309 ichnofabric dominated by horizontal burrows filled by bioclastic sands. D) “Columnar burrow set”. E)
1310 Coarse-fill burrows ichnofabric overlain by sand-mud couplets pertaining to the ichnofabric group 2.
1311
1312 **Figure 12.** A) Scolicids ichnofabric overlying the sand/mud couplets typical of the ichnofabric group 2.
1313 B) Close-up of A showing a specimen of *Scolicia* reworking a mud layer. *Palaeophycus* and *Planolites*
1314 are present in the sand layer, whereas “sharp-walled traces” bioturbates the mud layer. C) Scolicid. D)
1315 *Palaeophycus* ichnofabric with a large specimen of *Teichichnus* (morphotype A) and *Palaeophycus*. E)
1316 *Palaeophycus*. F) *Rosselia*? G) High bioturbation ichnofabric. H) Close-up of G showing a probable
1317 specimen of *Asterosoma*. I) High bioturbation ichnofabric with a distinct *Teichichnus* (morphotype B).
1318 L) High bioturbation ichnofabric with distinct lined vertical burrows (*Schaubcylindrichnus*?)

1319
1320 **Figure 13.** Environmental evolution of the Arda Section. A simplified stratigraphic log (sed. log) with
1321 the age of the section, based on calcareous nannofossil (CNZ) and foraminifera (FZ) biostratigraphy, is
1322 illustrated (Crippa et al., 2016). For each tool used (Sed: sedimentology; Body: body fossils; Trace:
1323 trace fossils) it was analysed: *Water depth*: 1. Foreshore (region between high tide water level and the
1324 low tide water level), 2. Shoreface (low tide water level-fair weather wave base), 3. Offshore transition
1325 and deeper (wave base-shelf edge break; Nichols, 2009). In the modern Adriatic Sea, these regions are
1326 respectively at depths of <0 m, 0-10 m, >10 m. *Energy*: 1. Low (nutrients in deposition), 2. High and
1327 fluctuating (hyperpycnal flows), 3. High (nutrients in suspension). *Sedimentation rate*: 1. Low, 2. High.
1328 *Oxygenation*: 1. Disoxic (2-0.2 ml O₂/l H₂O), 2. Oxic (8.0-2.0 ml O₂/l H₂O) (Tyson and Pearson, 1991;
1329 Buatois and Mangano, 2011, p.104). *Salinity*: 1. Brackish (0.5-30 ‰), 2. Seawater (30-40 ‰) (Buatois
1330 and Mangano, 2011, p. 107). *Water temperature*: 1. Cold, 2. Temperate, 3. Warm. For body fossils,
1331 water temperature was based on oxygen isotope composition of bivalve shells, considering cold: > 2.5
1332 ‰, temperate: 0-2.5 ‰, warm: < 0 ‰ (data from Crippa et al., 2016). For trace fossils, climate is

1333 defined as following: cold (climate at modern arctic to temperate latitudes), temperate (climate at
1334 modern temperate to tropical and subtropical latitudes) and warm (climate at modern tropical and
1335 subtropical latitudes). Arctic latitudes are between 66° and 90°, temperate latitudes are between 35°
1336 and 66°, tropical and subtropical latitudes are between 0° and 35° (Goldring et al., 2004, 2007).

1337

1338 **TABLE CAPTIONS**

1339

1340 **Table 1.** Facies classification scheme utilised for the Arda section following the genetic classification
1341 proposed by Zavala et al. (2011). All these facies categories are genetically related and occupy a
1342 definite position within the hyperpycnal system. The B facies is diagnostic of proximal areas and
1343 progressively disappears as the flow enters the area of lobe deposition. The S facies is the consequence
1344 of the loss of flow capacity and is typical of the medium to distal parts of the system. The L facies
1345 results from the flow inversion, which is diagnostic of flow-margin areas (both down the depositional
1346 axis and laterally along the axis).

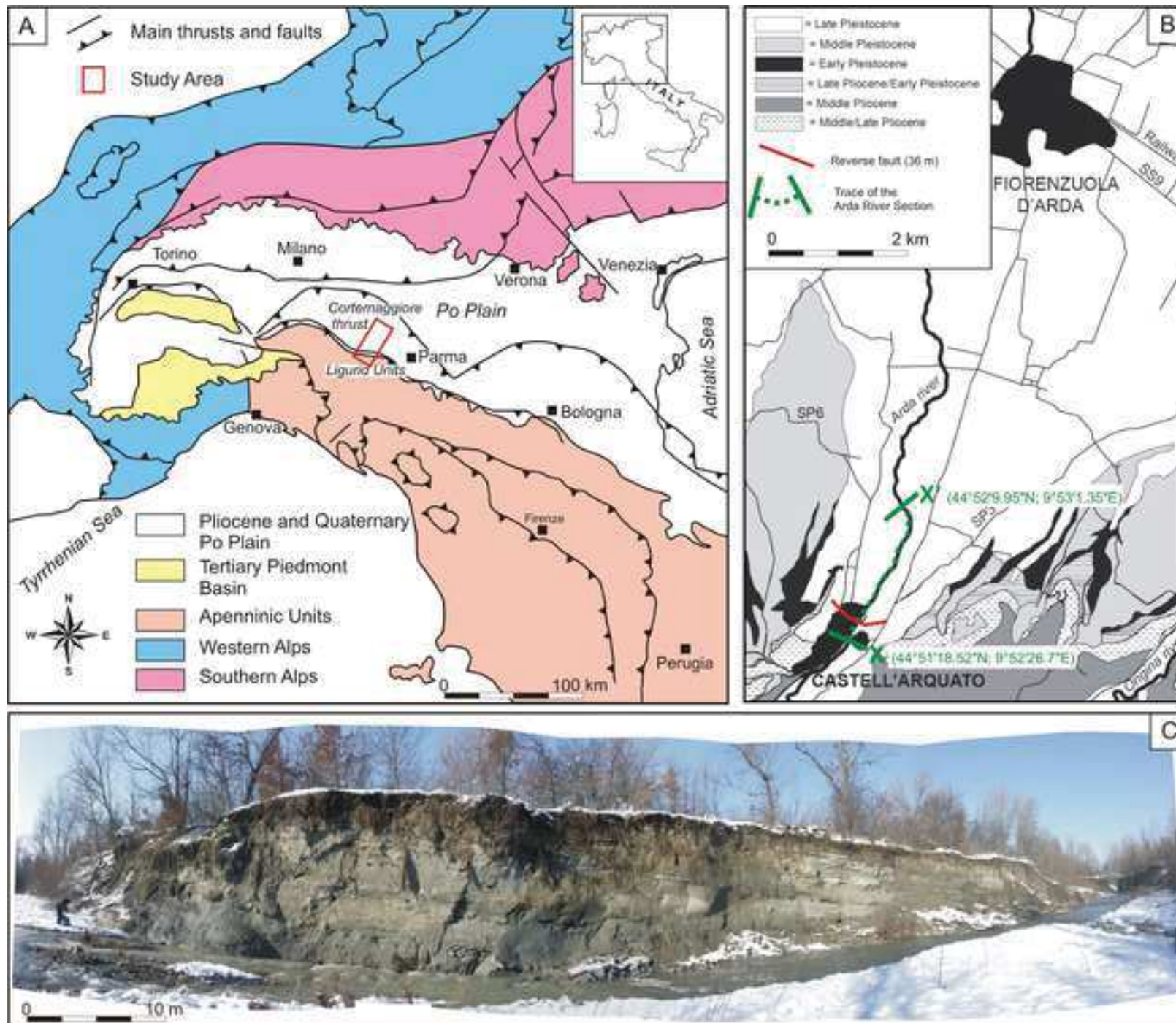
1347

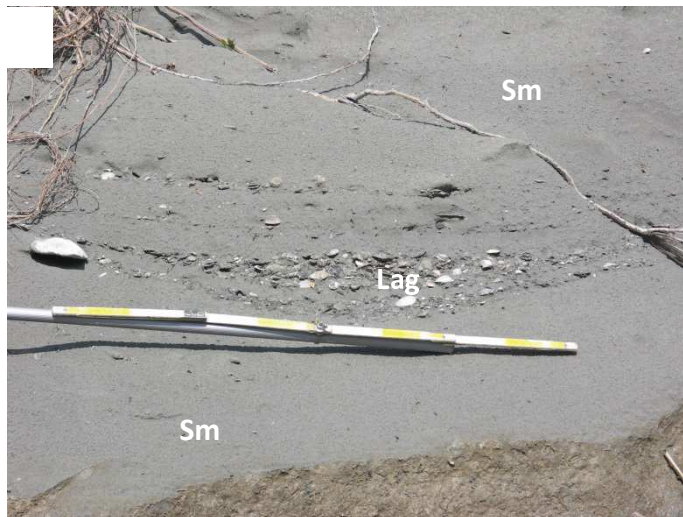
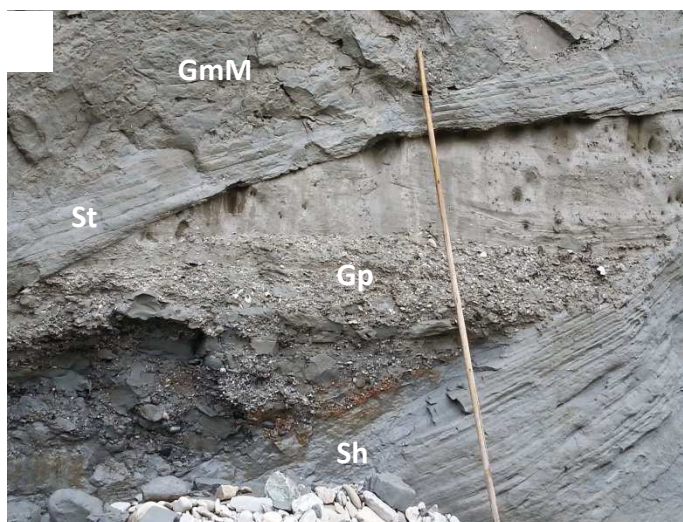
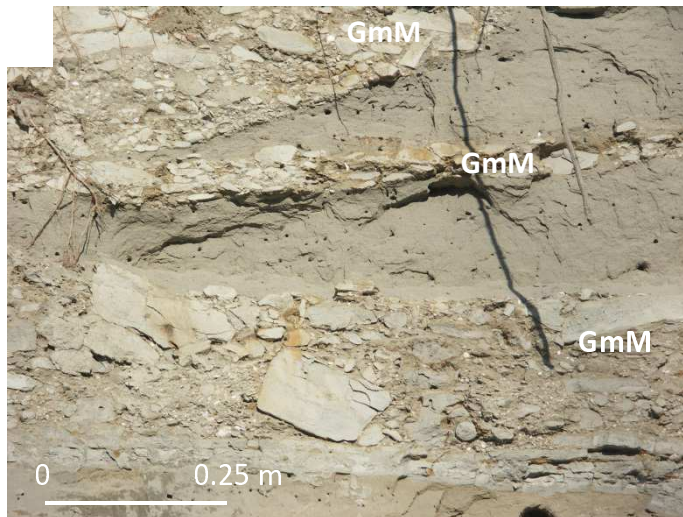
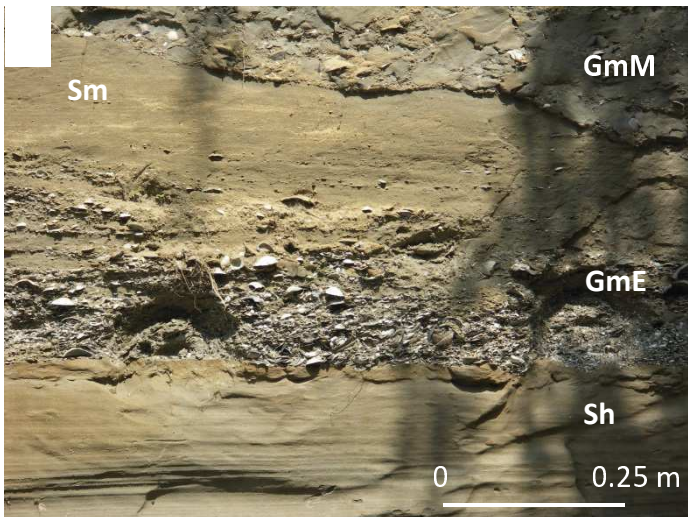
1348 **Table 2.** Ichnofabrics of the Arda river. Ichnotaxa are described in Table A2 in the Supplementary
1349 information online. The degree of bioturbation is quantified by the ichnofabric index (ii) (Bottjer and
1350 Droser, 1991). Firm substrates indicate stiffgrounds (Wetzel and Uchman, 1998) and firmgrounds
1351 (Fürsich, 1978; Bromley, 1996). Diversity refers to the typical number of distinct burrows per sampling
1352 unit. All ichnofabrics indicate oxic settings.

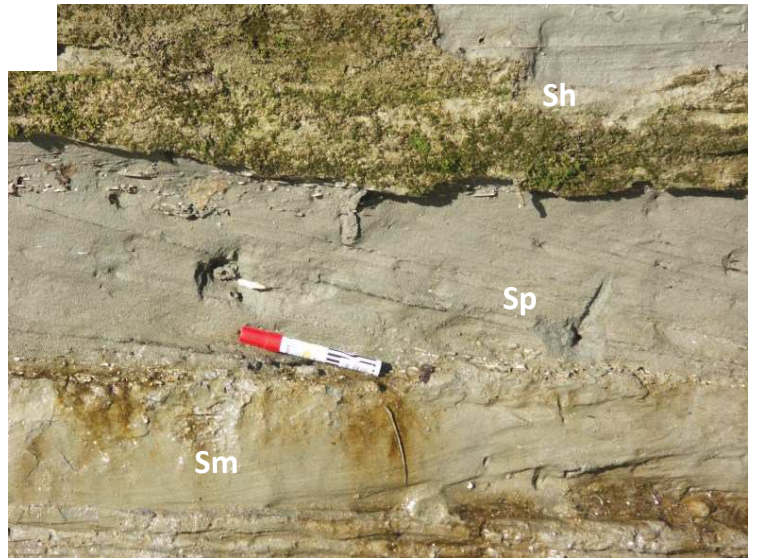
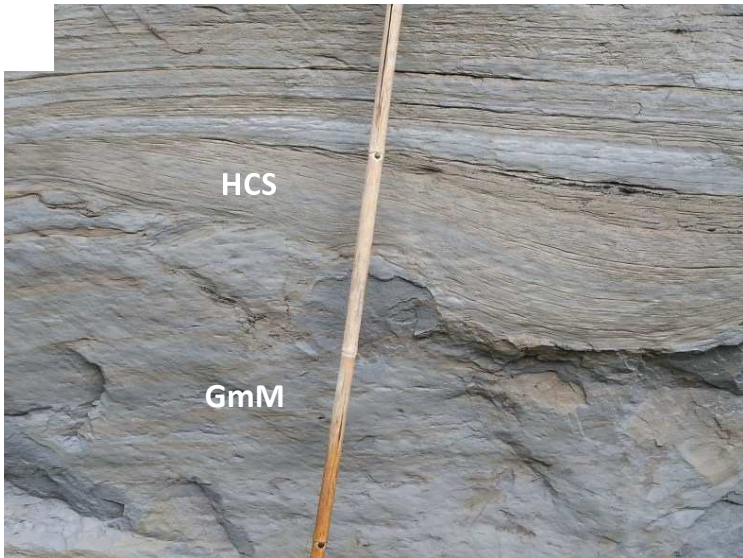
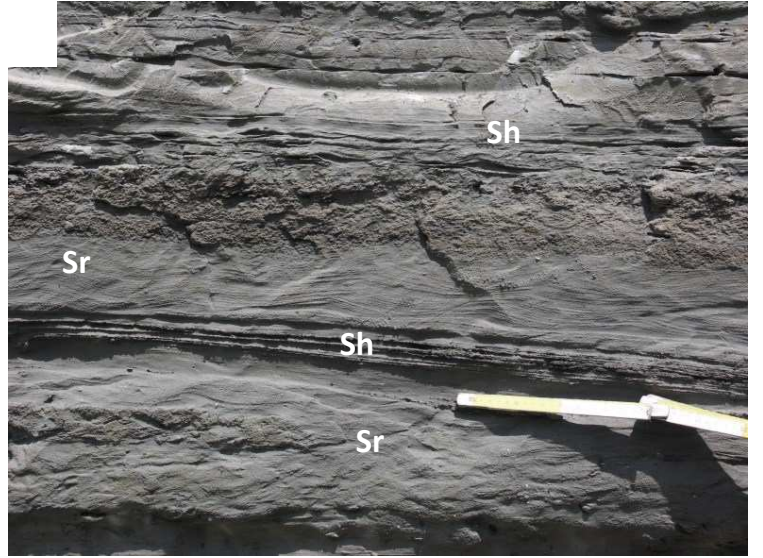
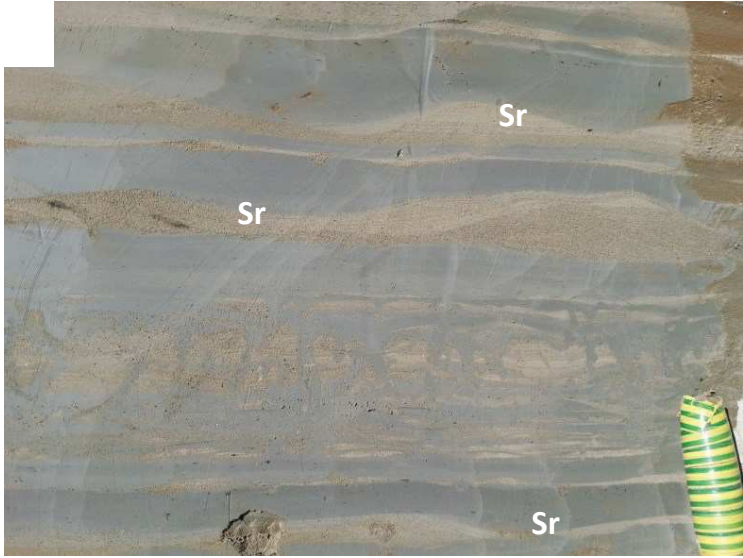
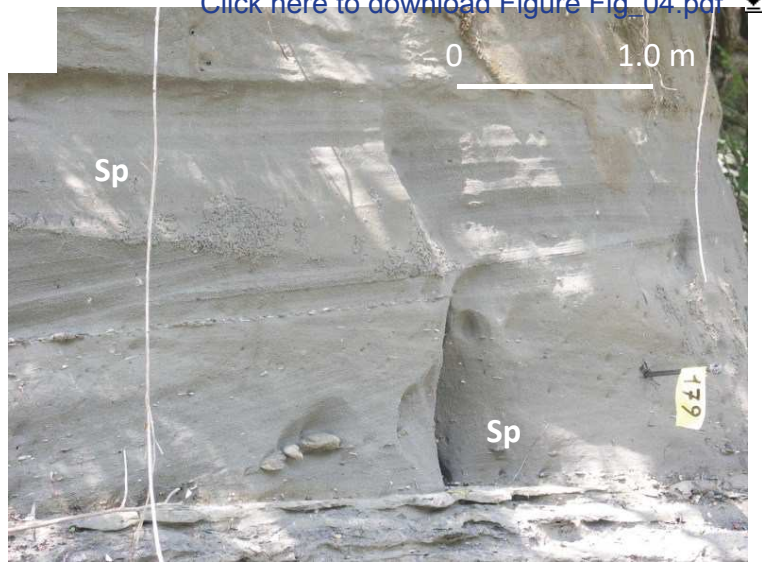
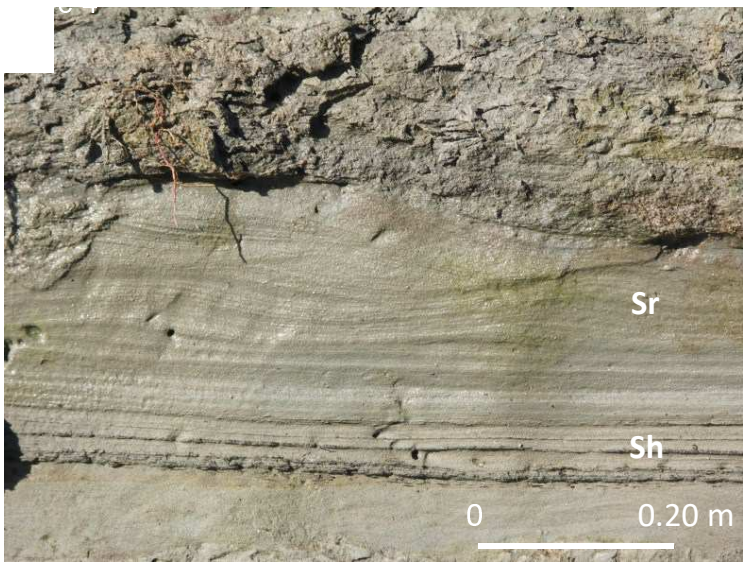
1353

1354

1355







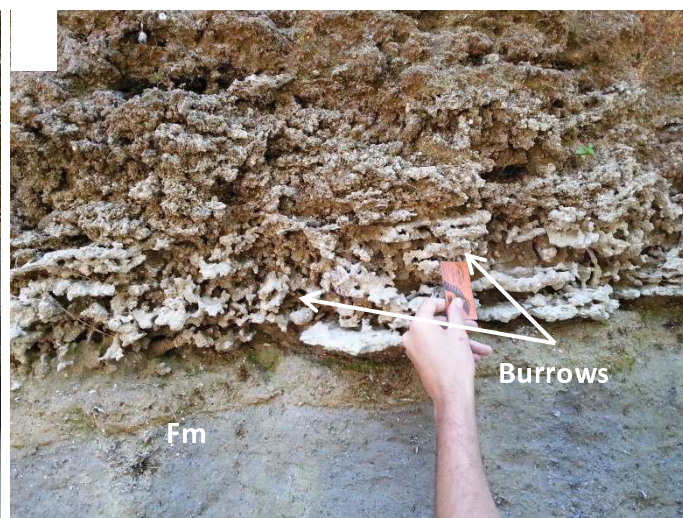
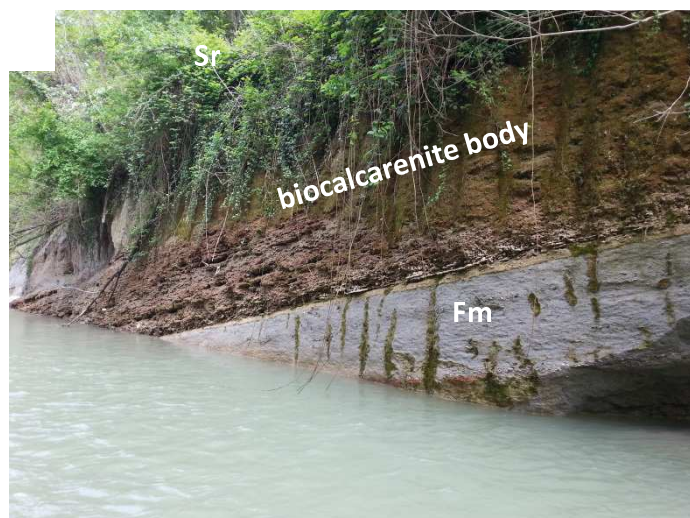
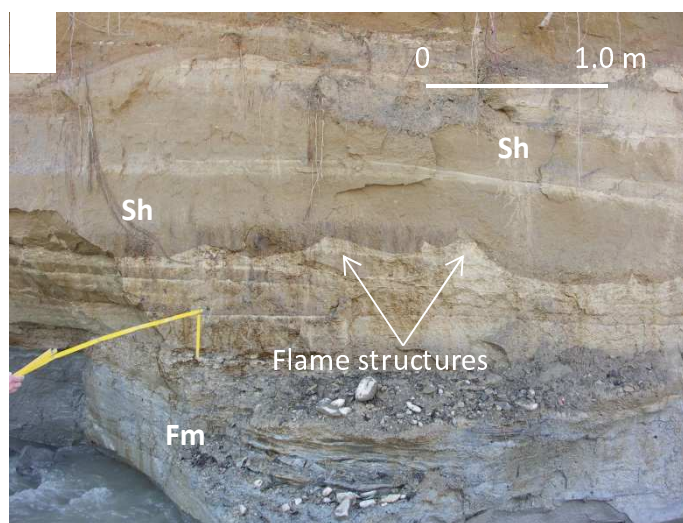
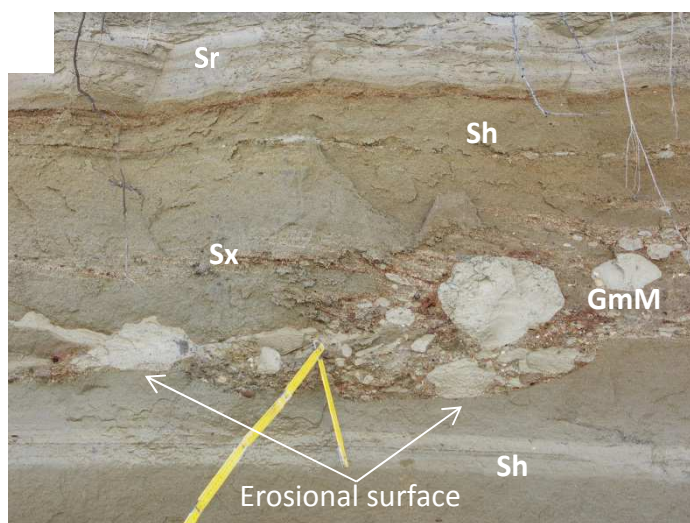
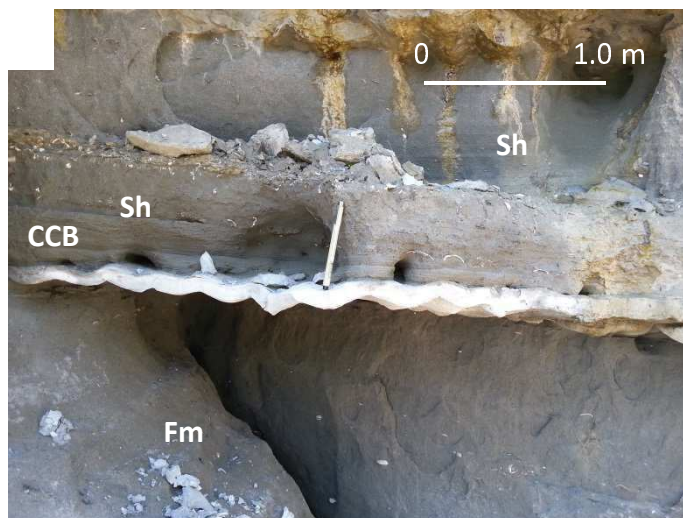
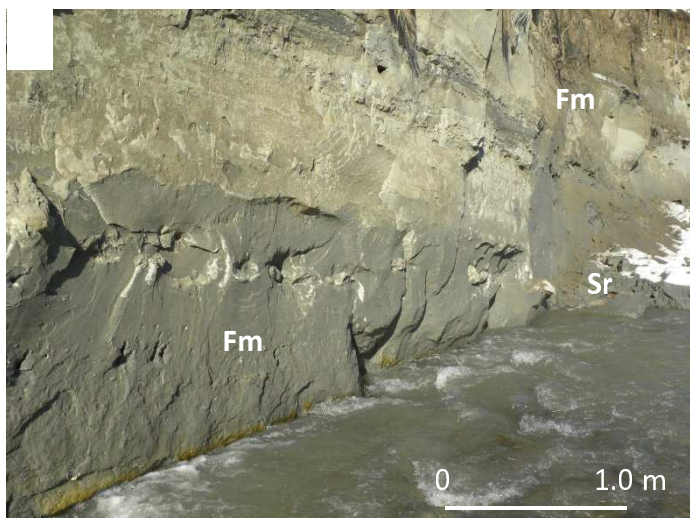




Figure 7

[Click here to download Figure Fig_07 bf.jpg](#)



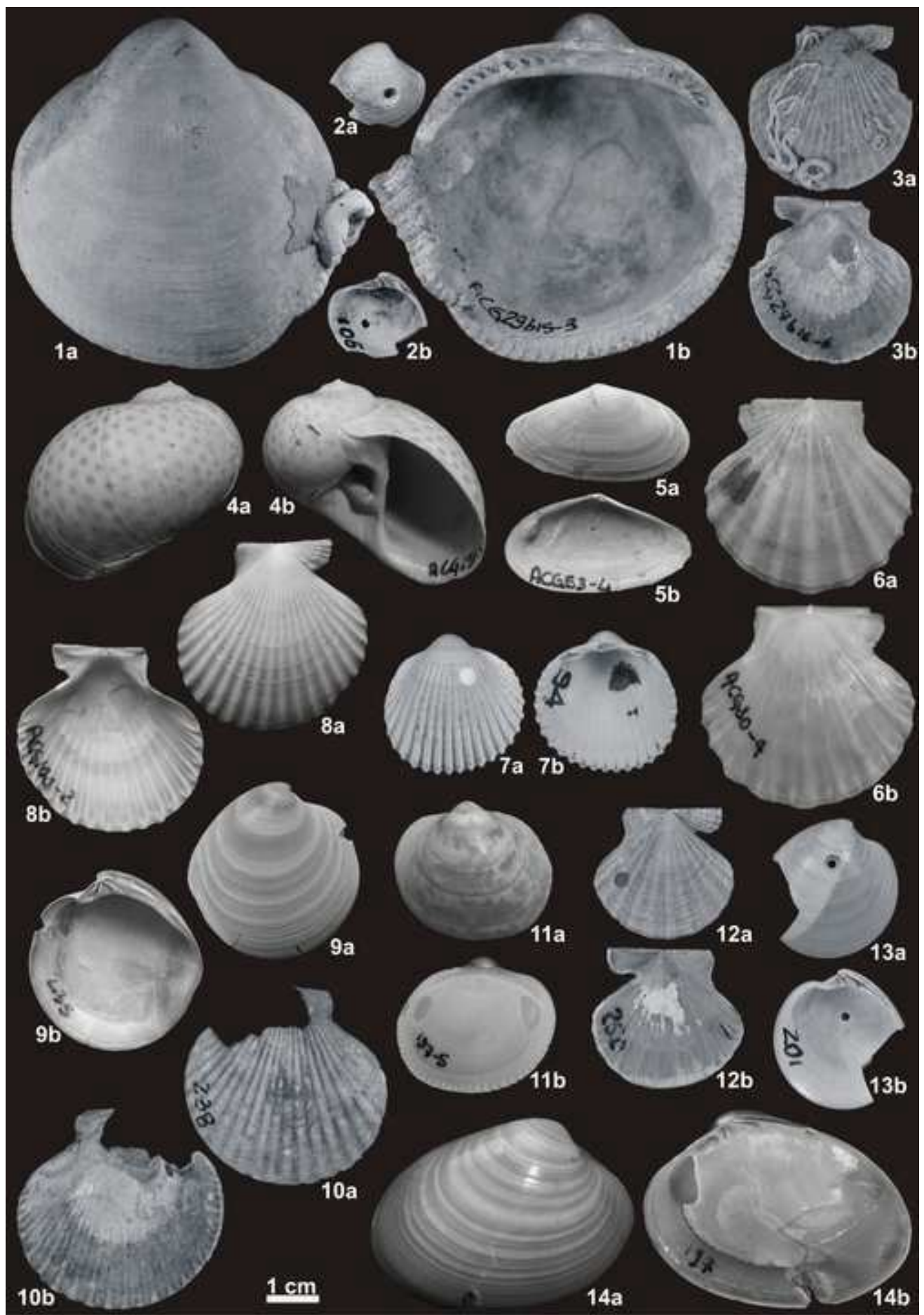
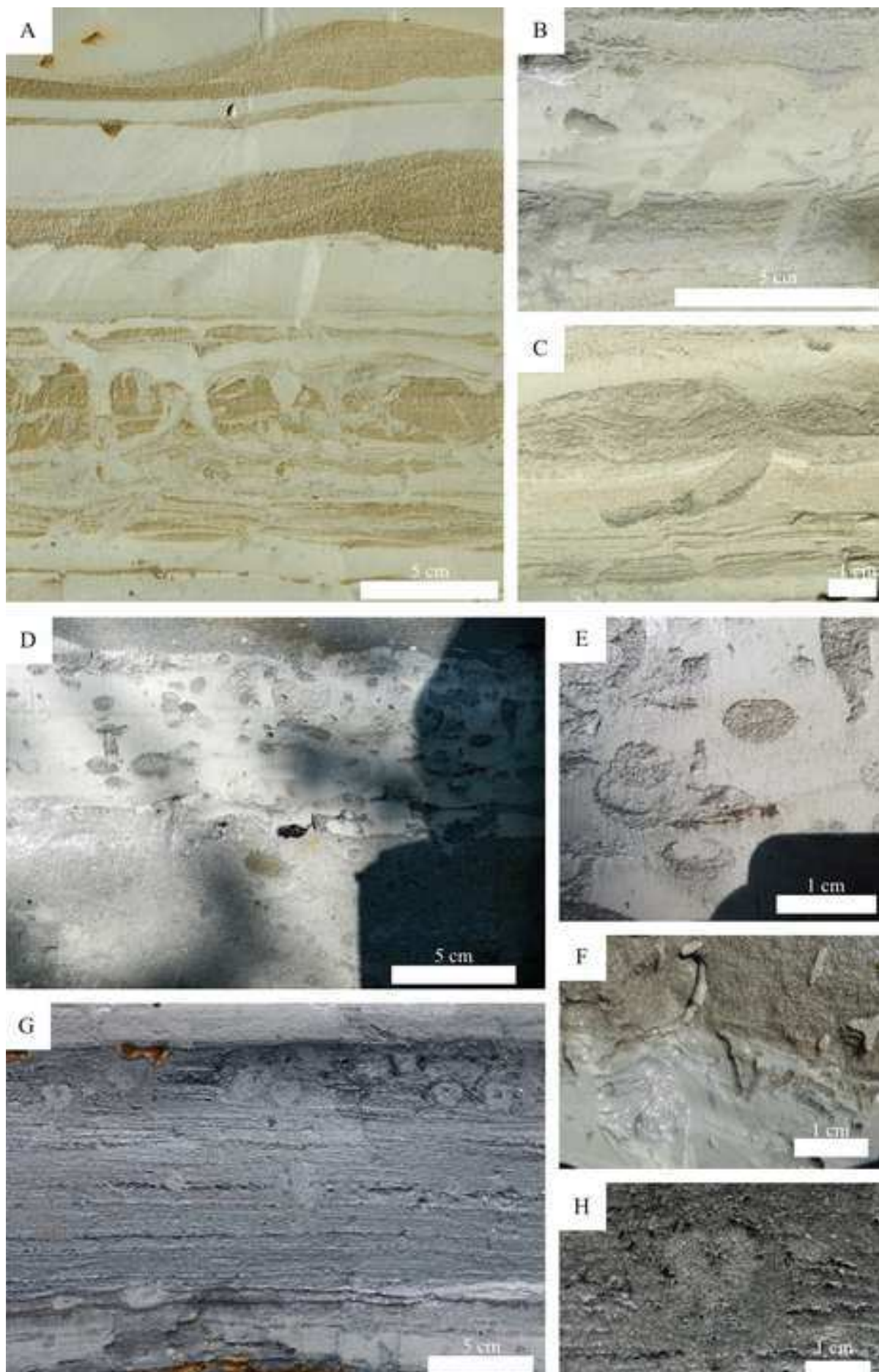
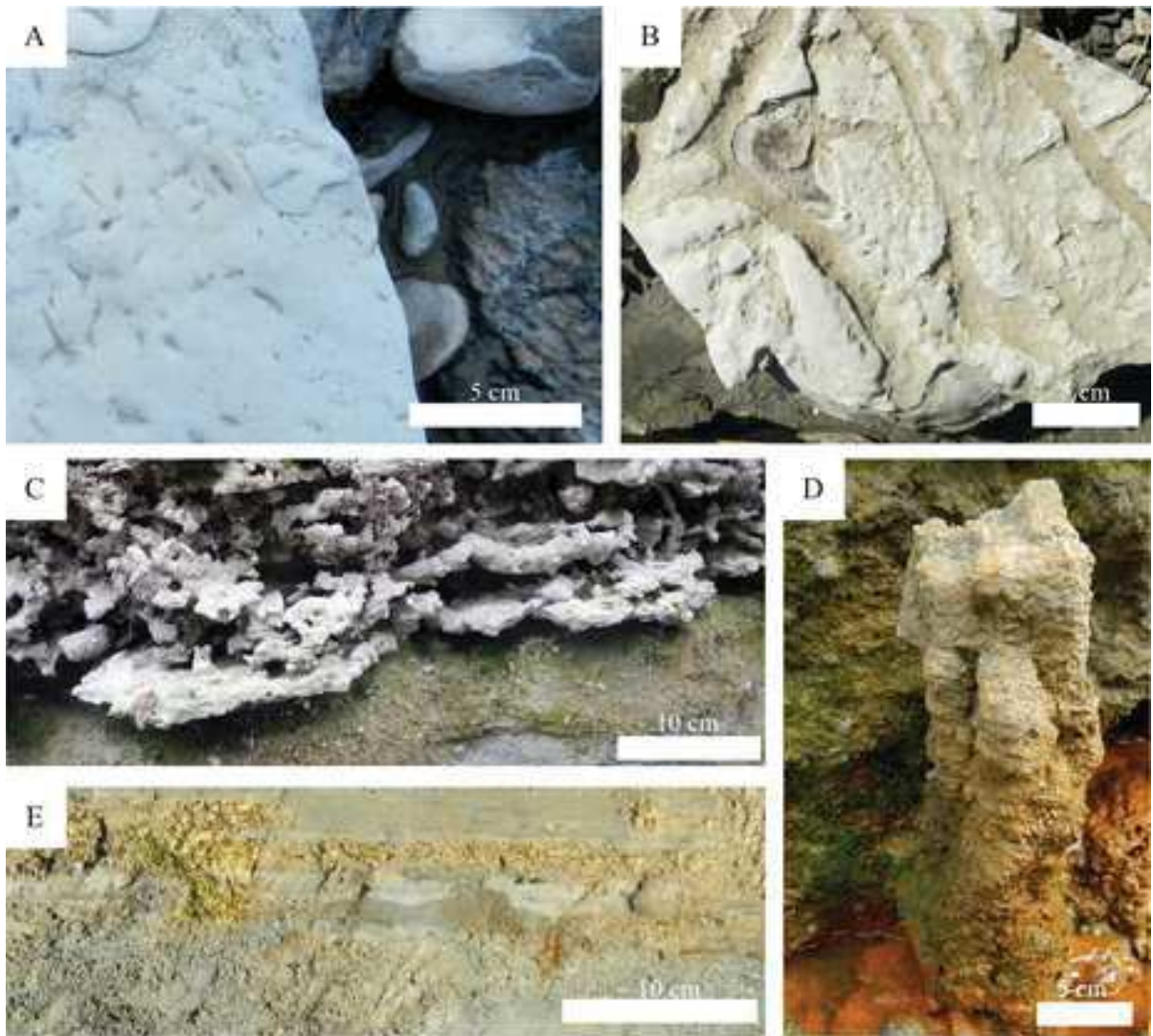


Figure 9

[Click here to download Figure Fig_9 tf.jpeg](#)







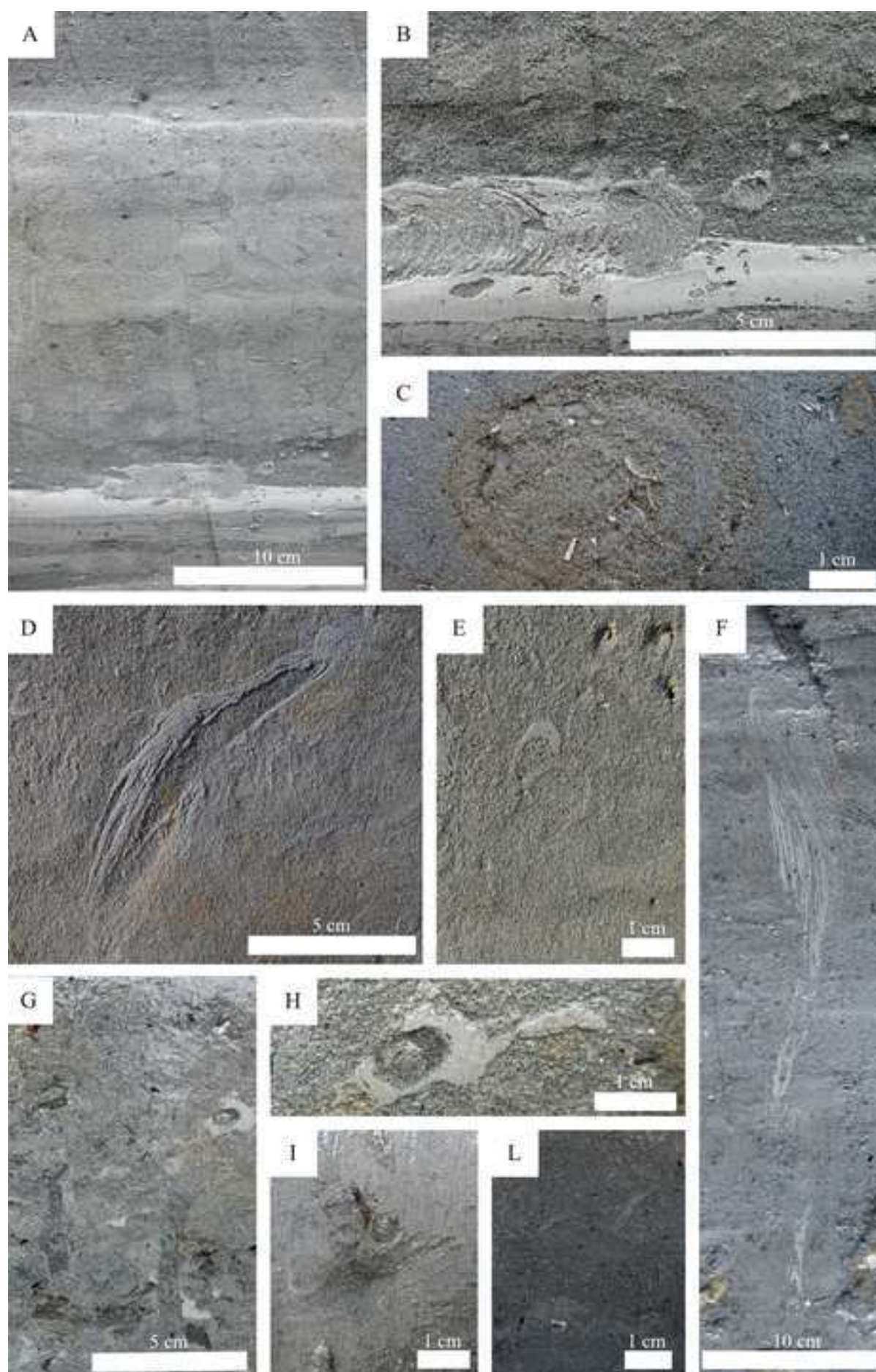


Figure 13

[Click here to download Figure Fig_13.pdf](#)

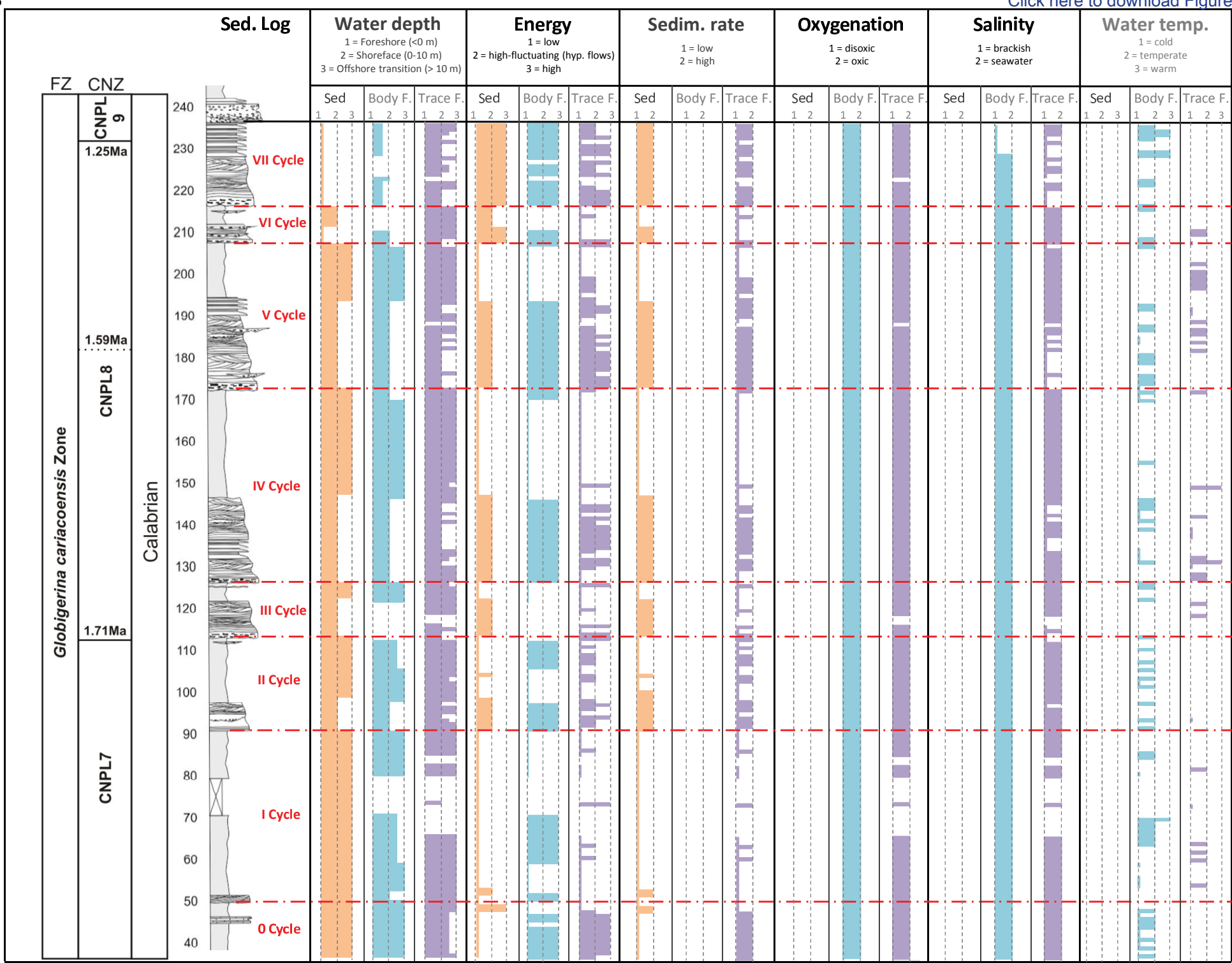


Table 1

Facies categories	Code	Facies	Sedimentary features
Facies B (bed-load related)	GmE	<i>Massive grain-supported gravels</i>	Massive, grain supported polygenic gravels. Beds have an erosive base and are usually heavily cemented (Fig. 3 A).
	GmM	<i>Massive mud clasts deposits</i>	Massive rip-up clasts deposits. Sandy matrix with abundant bioclasts (bivalves and gastropod shell fragments). Beds have an erosive base. Mud clasts are ripped from muddy layers (Fig. 3 A, B, D; Fig. 4 E; Fig. 5 C).
	Gp	<i>Planar stratified gravels</i>	Gravels with horizontal or oblique planar stratification. Clasts are usually embriated. Some of these beds are heavily cemented (Fig. 3 D).
	Lag	<i>Lag deposits</i>	Gravel carpets with bioclastic and sandy (very coarse) matrix (Fig. 3 E).
Facies S (suspended-load-related)	Sp	<i>Planar oblique stratified sands</i>	Mostly bioclastic, planar oblique stratified coarse grained sands. Beds are heavily cemented and bioturbated. Bioturbation is in the form of vertical tunnels (Fig. 4 B, F).
	Sx	<i>Planar cross stratified sands</i>	Fine to medium grained planar cross stratified sands. Bioturbation is apparently absent (Fig. 5 C).
	HCS	<i>Hummocky cross stratified sands</i>	Fine to coarse grained hummocky stratified sands. Beds are usually rich in bioclasts. Bioturbation is apparently absent. Occurrence of wood fragments and logs. (Fig. 4 E).
	St	<i>Trough cross stratified sands</i>	Fine to coarse grained trough cross stratified sands. Beds are usually rich in bioclasts. Bioturbation is apparently absent. Occurrence of wood fragments and logs (Fig. 3 C, B).
	Sr	<i>Ripple cross stratified sands</i>	Fine grained sands with wave or current ripples, sometimes with well-developed climbing ripples laminasets(current). No evidence of bioturbation (Fig. 4 A, B, D; Fig. 5 A, C).
	Sh	<i>Horizontally stratified sands and silts</i>	Horizontally stratified fine and very fine grained sands and silts usually rich in organic matter (small wood fragments) and mollusc fragments (Fig. 3 A, C, D; Fig. 4 A, D, F; Fig. 5 B, C, D).
	Sm	<i>Massive sands</i>	Very fine to medium grained massive sands. Beds are locally bioturbated (Fig. 3 A, E, F; Fig. 4 F; Fig. 5 C).
	HeB	<i>Heterolitic bedding</i>	Heterolitic fine grained sands to mud. Flaser, wavy and lenticular bedding.
Facies L (lofting-related)	Fm	<i>Massive fines</i>	Structureless silts and muds with minor very fine sands. Beds are locally heavily bioturbated. Presence of in-life position marine bivalves in the lower part of the stratigraphic section. In the upper part (continental deposits) frequent root systems and vertebrates (Fig. 5 A, B, E, F).
	CCB	<i>Carbonatic Cemented Beds</i>	Cemented levels, rich in carbonate. (Fig. 5 B)

Ichnofabric group	Ichnofabric class	Degree of bioturbation (ii)	Data					Interpretation		
			Characteristic ichnotaxa	Accessory components	Diversity (n)	Facies	Figures	Depositional environment	Major environmental features	Climate
1	Unbioturbated ichnofabric	1	-	-	0	GmE, Gp	-	Fluvial	-	-
	Low bioturbation ichnofabric	1-2	<i>Planolites</i> , <i>Palaeophycus</i> , cryptobioturbation	-	0-1	Sx, St, Sr	-	Foreshore-middle shoreface	Brackish water	-
	<i>Skolithos</i> ichnofabric	2	<i>Skolithos</i>	-	1	Sm	-	Backshore?; Foreshore-upper shoreface	-	-
	<i>Ophiomorpha</i> ichnofabric	2	<i>Ophiomorpha</i>	<i>Macaronichnus</i>	1	Sh	9 A-C	Foreshore-shoreface	High energy	Warm
	<i>Macaronichnus</i> ichnofabric	4-5	<i>Macaronichnus</i>	"Lined light filled burrows", "unlined light filled burrows"	1	Sm	9 D-F	Foreshore-shoreface	High energy	Temperate-cold
2	Few sharp burrows – smooth burrows ichnofabric	1-2	<i>Bergaueria</i>	Fugichnia	0-1	HeB	10 A-C	Upper shoreface-offshore	Hyperpycnal-influenced, rhythmical development of firm substrates	-
	Sharp burrows – Scolicids ichnofabric	2-3	Scolicids (<i>Scolicia</i> , <i>Bichordites</i>)	<i>Palaeophycus</i> , <i>Planolites</i> ?, <i>Thalassinoides</i> , oblique burrows, <i>Teichichnus</i> -like, mantle and swirl structures	1-3	HeB	10 G-H	Upper shoreface-offshore	Hyperpycnal-influenced, rhythmical development of firm substrates	Warm
	Sharp burrows – smooth burrows ichnofabric	2-3	"sharp-walled burrows"	mottles, dark-filled <i>Planolites</i> , <i>Scolicia</i> , <i>Schaubcylindrichnus</i> ? (morphotype A), <i>Planolites</i> , <i>Palaeophycus</i> , <i>Rosselia</i> ?, <i>Teichichnus</i>	1-5	HeB	10 D-F	Offshore	Hyperpycnal-influenced, rhythmical development of firm substrates	-
3	<i>Lockeia</i> ichnofabric	2-3	<i>Lockeia</i> , <i>Ophiomorpha</i> , <i>Siphonichnus</i> , <i>Arenicolites</i> , <i>Diplocraterion</i> , <i>Skolithos</i>	"winding trails"	0-1	CCB	11 A, B	Foreshore?	Firm substrates	-
	<i>Thalassinoides</i> ichnofabric	3-5	<i>Thalassinoides</i>	"Y-shaped burrows", "columnar burrow sets"	1	Sp	11 C, D	Shoreface?	High energy	-
	Coarse-fill burrows ichnofabric	4-5	"Coarse-fill burrows"	-	1	Fm	11 E	Submarine canyon?	Firm substrates	-
4	<i>Scolicids</i> ichnofabric	4-5	<i>Scolicids</i> (<i>Scolicia</i> , <i>Bichordites</i>)	-	1-3	Sm, Fm	12 A-C	Lower shoreface - offshore	Hyperpycnal-influenced?	Warm
	<i>Palaeophycus</i> ichnofabric	5-6	<i>Planolites</i> , <i>Palaeophycus</i> , <i>Schaubcylindrichnus</i> ? (morphotype A), <i>Scolicia</i> , <i>Rosselia</i> ?, <i>Teichichnus</i> (morphotype A).	-	3	Sm, Fm	12 D-F	Offshore	-	-
	High bioturbation ichnofabric	5-6	Dark-filled <i>Planolites</i> , <i>Schaubcylindrichnus</i> ? (morphotype A), <i>Palaeophycus</i> , <i>Teichichnus</i> (morphotype B), <i>Asterosoma</i> .	bioerosion traces (<i>Oichnus</i> , <i>Entobia</i> ?), "shell filled burrows"	0-3	Fm	12 G-L	Offshore	-	-